FAIRSEA (ID 10046951)

"Fisheries in the AdriatIc Region - a Shared Ecosystem Approach"

D 4.2.1 – Production patterns in the Adriatic Sea

Work Package:	WP4 **Implementation of a shared and integrated platform** Activity: 4.2 - **BGC – Biogeochemical processes and dynamics**
Type of Document	A report and a database on the space-time distribution of nitrogen, chlorophyll, primary production, plankton biomass and oxygen indicators for the past 20 years
Use	Public
Responsible PP	LP-OGS
Authors	Gianpiero Cossarini, Marco Reale, Vinko Bandelj, Paolo Lazzari, Anna Teruzzi [LP-OGS]
Version and date	Version 1, 31/12/2019

Deliverable 4.2.1

Production patterns in the Adriatic Sea

FAIRSEA – Fisheries in the Adriatic Region – a shared Ecosystem Approach

FAIRSEA is financed by Interreg V-A IT-HR CBC Programme (Priority Axis 1 – Blue innovation)

Start date: 01 January 2019

End date: 28 February 2021

Contents

Acronyms used

BFM	Biogeochemical Flux Model
CMCC	Centro Euro-Mediterraneo per i Cambiamenti Climatici
CMEMS	Copernicus Marine Environment Monitoring Service
DIC	Dissolved Inorganic Carbon
DIN	Dissolved Nitrogen
EAF	Ecosystem Approach to Fisheries
EAFM	Ecosystem Approach to Fisheries Management
ESA-CCI	ESA-Climate Change Initiative
FAIRSEA	Fisheries in the AdrIatic Region – a Shared Ecosystem Approach
GSA	FAO Geographical Sub Areas
HCMR	Hellenic Center for Marine Research
KoM	Kick-off Meeting
MFS	Mediterranean Forecasting System
NEMO	Nucleous for European Modelling of the Ocean
NetCDF	Network Common Data Form
OCTAC	Ocean Colour Thematic Assembly Centre
OGS	Istituto Nazionale di Oceanografia e di Geofisica Sperimentale
OGSTM	OGS - Transport Model
PFT	Plankton Functional Types
QUID	Quality Information Document
WP	Work packages

Introduction

This report presents a description of the biogeochemical properties of the Adriatic and Ionian basins (the physical properties are described in D 4.1.1). The analysis is based on the Copernicus physical and biogeochemical reanalysis, which covers the period 1999-2018. Data have a spatial resolution of 1/16° in the horizontal direction, while the vertical discretization is made of 72 unevenly-spaced levels (i.e., 3-5 m thick levels in the first 50 m; ~10 m at 100-150 m depth and 20-50 m between 200 and 2000 m). The data processed in the present report are freely available from the Copernicus Marine Environment Monitoring Service (hereafter CMEMS, http://marine.copernicus.eu). CMEMS provides regular and systematic core reference information on the (physical and biogeochemical) properties of the oceans and European regional seas. It is part of the EU COPERNICUS program, finalized to establish a European capacity for Earth Observation and Monitoring. Mediterranean reanalysis data are provided by the Mediterranean component of CMEMS (Med-MFC), which is an expert Centre for the ocean analyses and forecasts for the Mediterranean Sea composed by OGS (www.inogs.it), CMCC (www.cmcc.it) and HCMR (https://www.hcmr.gr/en/).

Data and figures of the present deliverable have been, respectively, reprocessed and generated specifically for the Adriatic and Ionian basins, using original CMEMS raw data downloaded from http://marine.copernicus.eu/services-portfolio/access-to-products/.

The Copernicus 1999-2018 reanalysis modelling system: the biogeochemical component

The present deliverable is the companion of deliverable D 4.1.1, describing the Copernicus Mediterranean physical-biogeochemical reanalysis modelling system. Only a brief summary of the Mediterranean CMEMS is depicted hereafter, focusing on its biogeochemical component.

The Copernicus physical and biogeochemical reanalysis covers the period 1999-2018. Data have a spatial resolution of 1/16°, which satisfies the requirements of the other WPs relying on hydrodynamic/biogeochemical output fields. Model domain is composed of 72 unevenly-spaced vertical levels at the depth of (from surface to bottom, in meters): 1.5, 4.6, 7.9, 11.6, 15.4,19.6333, 24.1, 28.9, 34.1, 39.7, 45.7, 52.1, 59.0, 66.4, 74.3, 82.8, 92, 101.7, 112.2, 123.4, 135.4, 148.3, 162.1, 176.8, 192.6, 209.4, 227.5, 246.8, 267.5, 289.6, 313.3, 338.6, 365.6, 394.5, 425.4, 458.5, 493.8, 531.6, 571.9, 615.1, 661.1, 710.3, 762.8, 818.9, 878.9, 942.8, 1011.2, 1084.1, 1161.9, 1245, 1333.6, 1428.2, 1529.1, 1636.6, 1751.3, 1873.5, 2003.8, 2142.7, 2290.6, 2448.2, 2615.9, 2794.6, 2984.7, 3186.9, 3402.1, 3630.7, 3873.8, 4132.1, 4406.5, 4697.7, 5006.8, 5334.648.

The dataset includes daily/monthly fields of 2D sea surface height and 3D temperature, salinity, meridional and zonal currents, chlorophyll-a, nitrate, phosphate, dissolved oxygen, phytoplankton carbon biomass, pCO_2, alkalinity, pH and net primary production. The domain encompasses the Mediterranean Basin (6°W-36.25°E and 30.1875°N-45.9375°N) and part of the Atlantic Ocean, in order to better resolve the exchanges at the Strait of Gibraltar. The physical model (NEMO coupled with the OceanVar assimilation scheme) is forced by momentum, water and heat fluxes interactively computed by bulk formulae using the 6-hours, 0.75° ERA-Interim reanalysis fields (Dee et al., 2011). Water

balance is computed as Evaporation minus Precipitation minus Runoff. The evaporation is derived from the latent heat flux, while the runoff is provided by monthly mean datasets: the Global Runoff Data Centre dataset (Fekete et al., 1999) for the Ebro, Nile and Rhone rivers and the dataset from Raicich (Raicich,1996) for the Adriatic rivers (Po, Vjosë, Seman and Bojana). The Black Sea is not included in the domain and thus, the Dardanelles inflow is parameterized as a river with net inflow rates taken from Kourafalou and Barbopoulos (2003). Precipitations are obtained from the ERA-Interim reanalysis (6-hours frequency, 0.75° horizontal resolution). The model assimilates satellite sea level anomaly and in situ temperature/salinity profiles.

The physical model provides the transport-biogeochemical reactor MedBFM1 with the temporal evolution of daily 3D fields of horizontal and vertical current velocities, vertical eddy diffusivity, potential temperature, salinity, in addition to surface data for solar shortwave irradiance and wind stress. The transport-biogeochemical reactor then simulates the dynamics of four plankton functional types (PFTs: diatoms, flagellates, picophytoplankton and dinoflagellates), zooplankton, the biogeochemical cycles of 4 chemical compounds (carbon, nitrogen, phosphorus and silica) through the dissolved inorganic, living organic and non-living organic compartments.

The Med-biogeochemistry system includes the data assimilation of surface chlorophyll concentration through a variational scheme (3DVAR-BIO, see details in Teruzzi et al., 2014). The surface chlorophyll concentrations are derived from satellite observations produced by OCTAC, based on the ESA-CCI data. The present version of 3DVAR-BIO assimilates chlorophyll concentration over the whole domain including both the open sea and coastal areas.

The biogeochemical component of the Mediterranean Reanalysis is provided by the OGS team and a detailed description can be found in the biogeochemical Quality Information

Document (QUID): http://marine.copernicus.eu/documents/QUID/CMEMS-MED-QUID-006-008.pdf

The QUID document provides also an assessment of the quality of the biogeochemical reanalysis based on the comparison with independent data (observational in-situ datasets), semi-independent data (satellite datasets) and literature estimates. The main results are reported below (for the main variables):

Chlorophyll: the model is able to capture spatial patterns, seasonal cycle and inter-annual variability. The bias is order 10^{-3} mg/m^3 in open sea while it increases to 10^{-1} mg/m^3 in coastal areas, with higher uncertainty and variability in the western sub-basins than eastern ones. In the coastal areas model underestimates the high values of chlorophyll-a.

Phytoplankton carbon biomass: consistency of the model formulation (discussed in several scientific papers) and validation of phytoplankton chlorophyll provide an indirect proof of the accuracy for this variable.

Phosphate: uncertainties at the basin scale are generally around 0.03 and 0.07 mmol/m^3 at the upper and deep layers, respectively while spatial gradients and vertical profile are consistent with observations.

Nitrate: spatial and vertical gradients are consistent with observations. Uncertainties at the basin scale are on the order of 0.5 and 1.5 mmol/m^3 at the surface and deep layers, respectively with higher uncertainties in the western Mediterranean Sea.

Oxygen: uncertainties are on the order of 10-15 mmol/m^3 at the basin scale, with western Mediterranean Sea areas affected by a not proper setting of the boundary conditions at the Atlantic buffer.

Net primary production: comparison with literature shows that the reanalysis simulation consistently reproduces basin-scale and sub-basin-scale estimates.

pH and pCO_2: the comparison with observations shows that the reanalysis satisfactorily reproduces the main spatial patterns and vertical dynamics of the carbonate system variables.

Biogeochemical characteristics of the Adriatic Sea and Northern Ionian Sea (GSA 17-18-19)

Data and methods

In this section we analyze the spatial patterns and temporal behavior of the biogeochemical properties in the Adriatic and Ionian systems. We consider annual and seasonal averages computed over the period 1999-2018. All the data elaborated in the present report have been downloaded from http://marine.copernicus.eu/ using an ad-hoc account created specifically for the FAIRSEA project by ASSAM (*Agency for Agrofood Sector Services of Marche Region)*, username*: fperretta*

We define the winter seasons as the period encompassing January-February-March (JFM), spring as the period encompassing April-May-June (AMJ), summer as the period encompassing July-August-September (JAS), fall as the period encompassing October-November-December (OND). The temporal averages have been computed considering the following vertical averaged levels: 0-50 m, 50-100 m, 100-200 m, 200-500 m and 500-800 m.

Dissolved Nitrogen

Fig.1 shows the mean annual dissolved inorganic nitrogen (DIN) concentration computed at the five aforementioned depths, while the corresponding seasonal averages are shown in Figs. 2, 3, 4 and 5. The distribution of surface DIN (0-50 m) clearly reflects the substantial discharge of nitrogen done by the rivers (mainly the Po River and the northern

Adriatic rivers) and the transport operated by coastal currents along the Italian coast, where the concentration is higher with respect to the rest of the domain. Relatively higher values of nitrogen concentration are observed between 50-100 m in the middle and southern Adriatic Pit, mostly associated with vertical mixing acting in the area in JFM and OND (as shown in Fig. 2 and Fig. 4). Moreover, moving along the water column, the concentration of nitrogen increases due to the accumulation of the nutrient below the photic depth. Comparing the monthly time-series of DIN at the surface, the Ionian is characterized by lower concentrations (in all the sub-areas and offshore zone, Fig. 6 and Fig. 8) with respect to southern and northern Adriatic, with the latter characterized by the highest values driven by river contribution. Considering only the inshore areas (Fig.7), due to the substantial river input at the surface, the northern Adriatic is characterized by the highest concentrations. The differences among the three sub-areas tend to fade when moving downwards along the water column. The amplitude of the seasonal cycle is higher in the Adriatic sub-basins, which are mostly influenced by the seasonality of river discharges and decreases with depth. Finally, a possible spurious spin-up effect affects the first few years of the simulation that depict a decreasing tendency, especially at the surface.

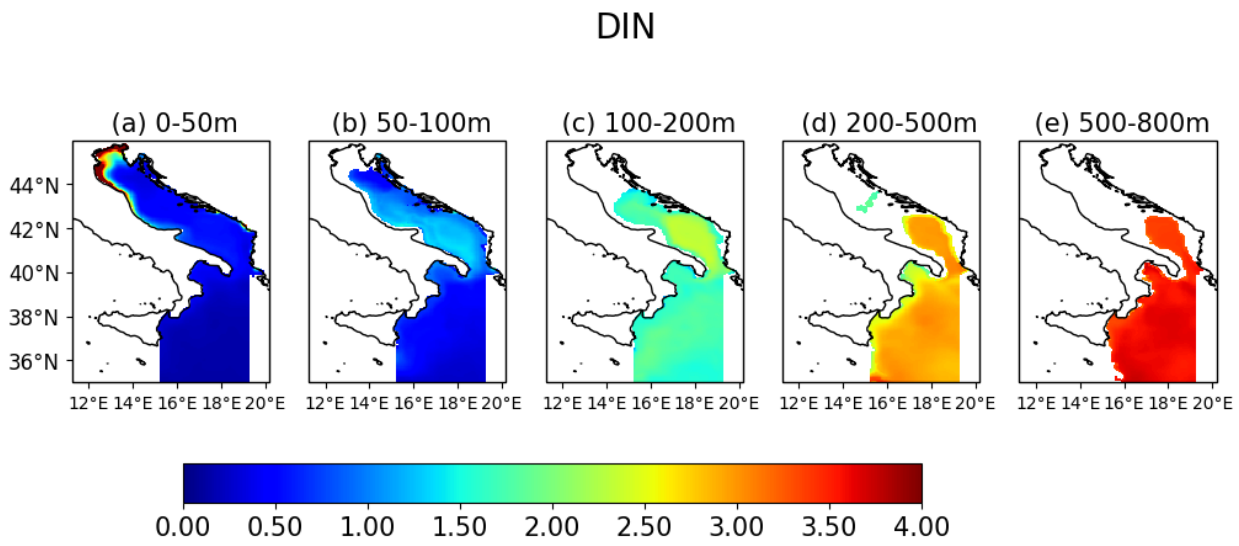

Figure 1 - Mean dissolved inorganic nitrogen concentration (mmol/m^3) in the period 1999-2018 in the layers between 0-50 m, 50-100 m, 100-200 m, 200-500 m and 500-800 m

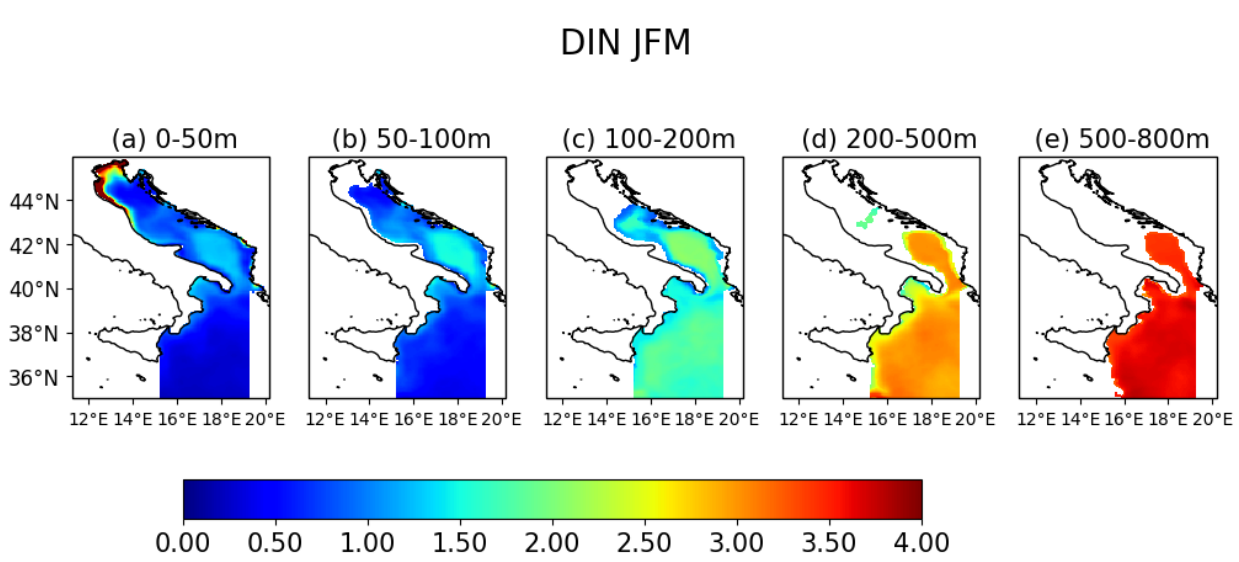

Figure 2 - Same as Fig. 1, but for January-February-March (JFM)

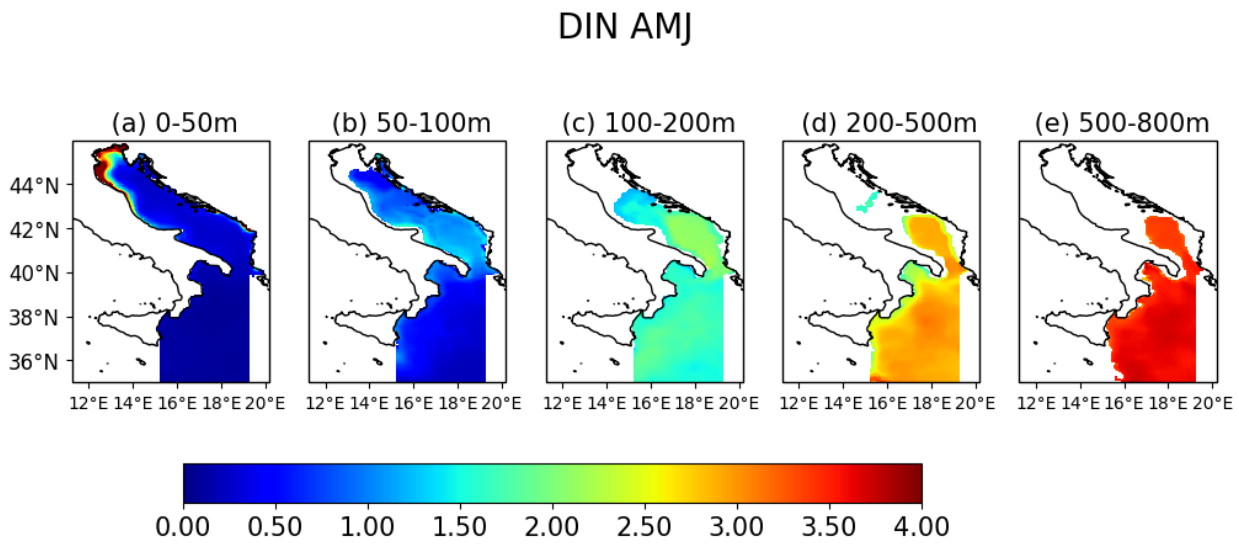

Figure 3 - Same as Fig. 2, but for April-May-June (AMJ)

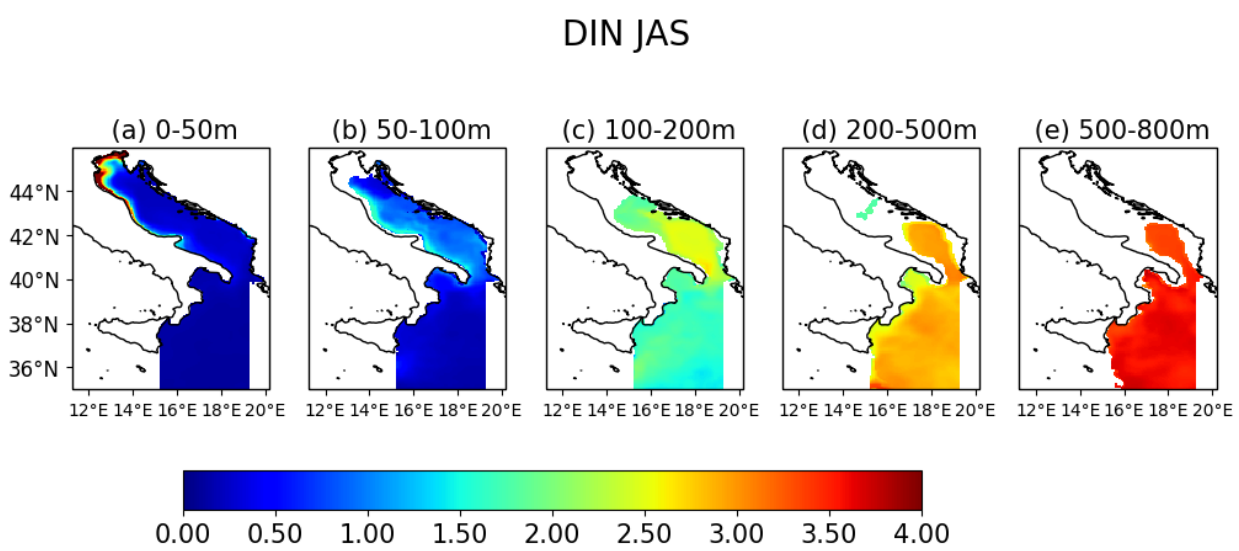

Figure 4 - Same as Fig. 3, but for July-August-September (JAS)

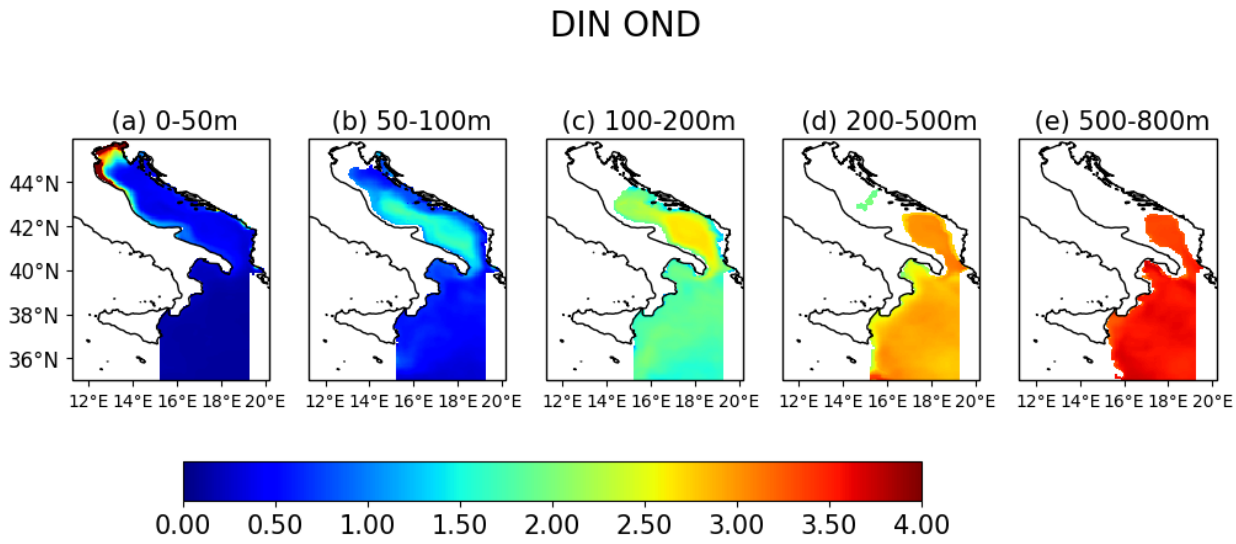

Figure 5 - Same as Fig. 4, but for October-November-December (OND)

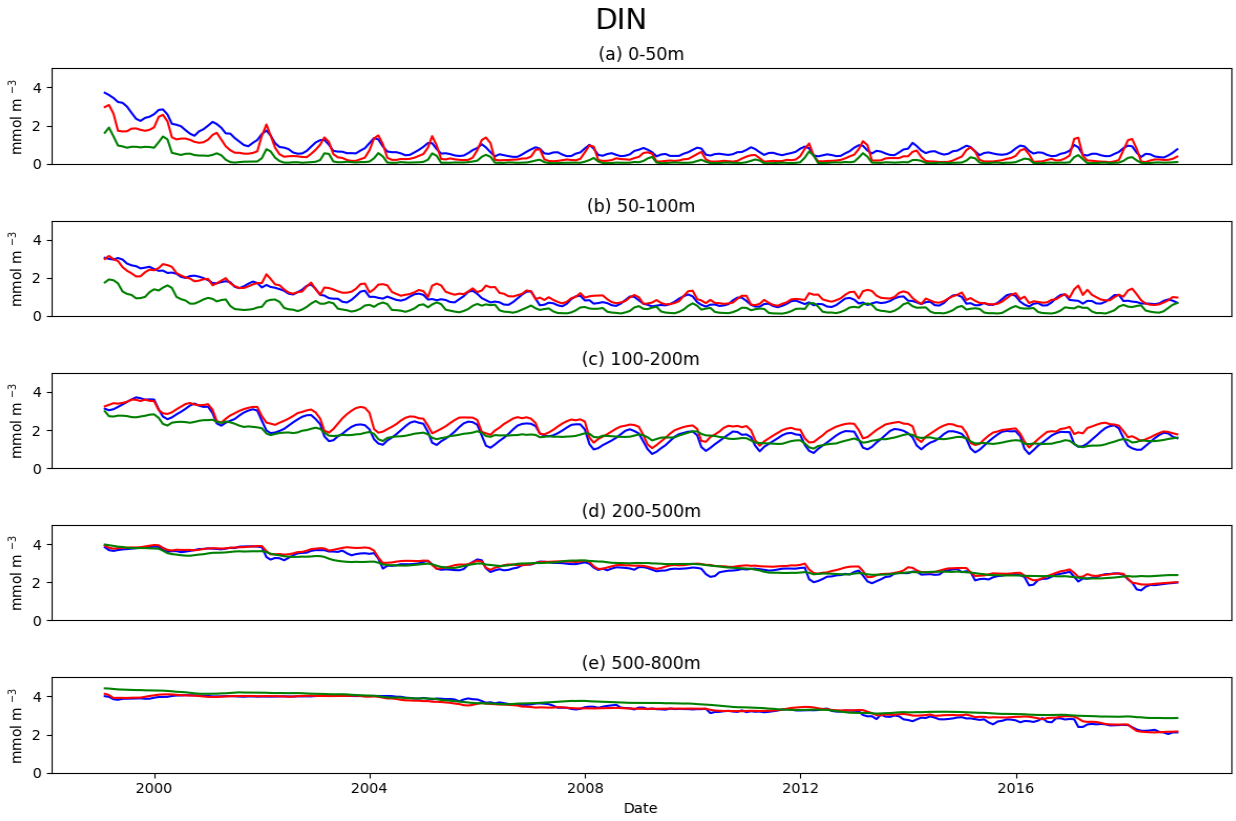

Figure 6 - Monthly timeseries of dissolved inorganic nitrogen (mmol/m^3) in the three sub-areas of the Adriatic-Ionian domain (ADR1: blue, ADR2: red and IONIAN: green) in the period 1999-2018

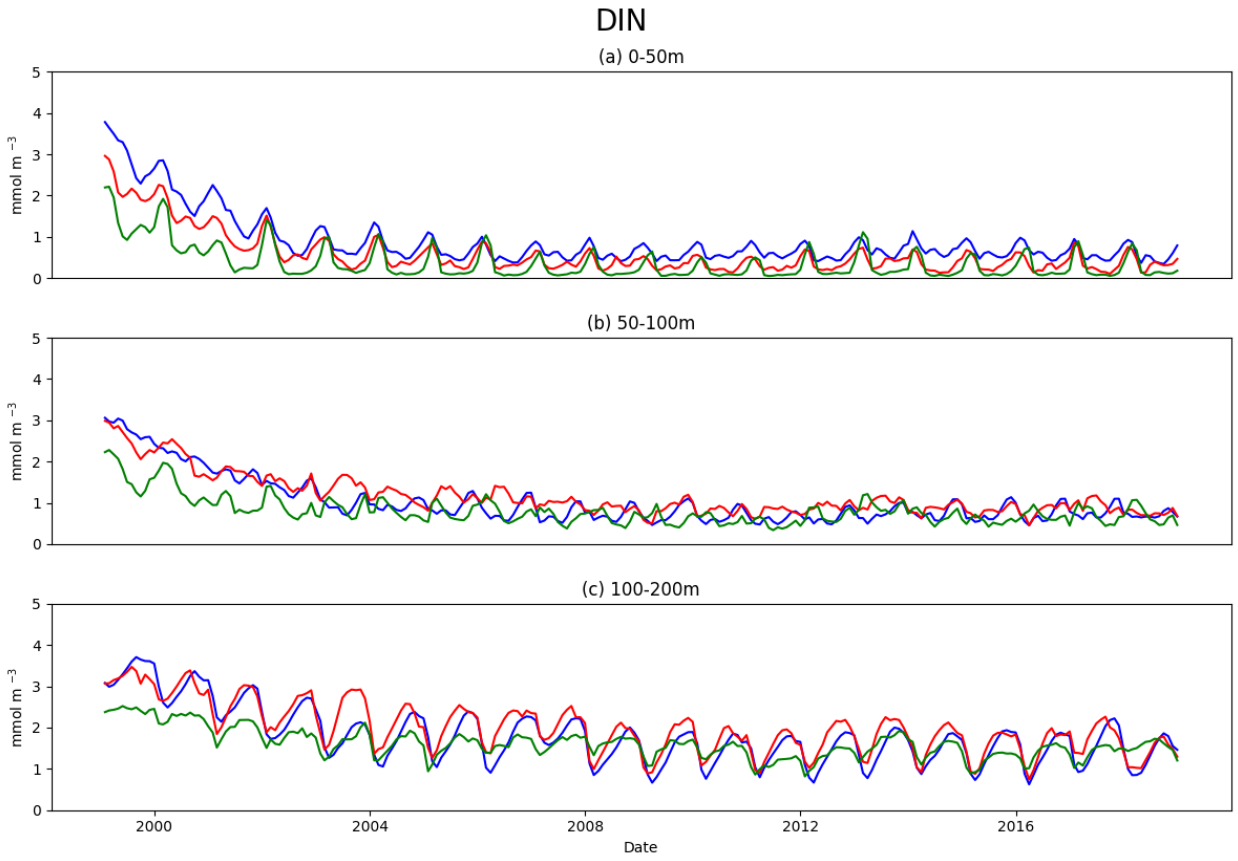

Figure 7 - Monthly timeseries of dissolved inorganic nitrogen (mmol/m^3) in the three inshore (depth less than 200 m) areas of the Adriatic-Ionian Sea (ADR1: blue, ADR2: red and IONIAN: green) in the period 1999-2018

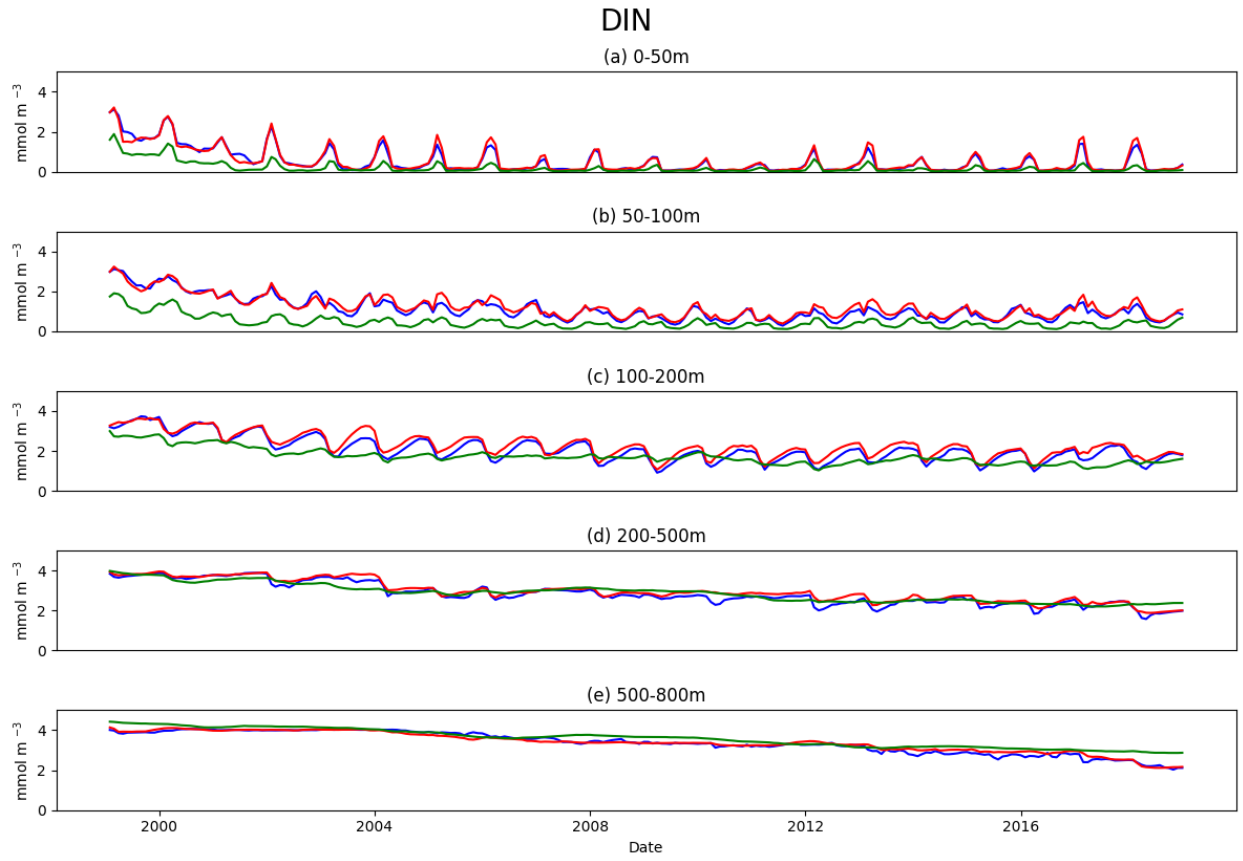

Figure 8 - Monthly timeseries of dissolved inorganic nitrogen (mmol/m^3) in the three offshore (deeper than 200 m) areas of the Adriatic-Ionian Sea (ADR1: blue, ADR2: red and IONIAN: green) in the period 1999-2018

Phosphate

Fig. 9 shows the mean annual phosphate concentration (PO_4) computed at the five aforementioned depths, while the corresponding seasonal averages are shown in Fig. 10, 11, 12 and 13. Phosphate is considered the limiting nutrient for phytoplankton growth in the Mediterranean Sea (Lazzari et al., 2012). The distribution of surface PO_4 (0-50 m) shows some similarities with that observed for the DIN. In fact, higher concentration are observed in the northern Adriatic at the mouth of the Po river. Further, higher values are simulated in the subsurface layers in the middle and southern Adriatic Pit. These patterns

are associated with the accumulation of the nutrient below the euphotic layer and with substantial vertical mixing occurring in the areas in JFM and OND (as shown in Fig. 10 and Fig. 13). Comparing the monthly time series of PO_4, the Ionian basin has still lower concentrations at the surface than the southern and northern Adriatic (Fig. 14 and Fig. 16). The differences between the three sub-areas tend to fade when moving downwards along the water column. Considering the inshore zones (Fig. 15), surface values show large seasonal oscillation with summer depletion, while subsurface layers are characterized by higher values in the Adriatic compared to the Ionian Sea.

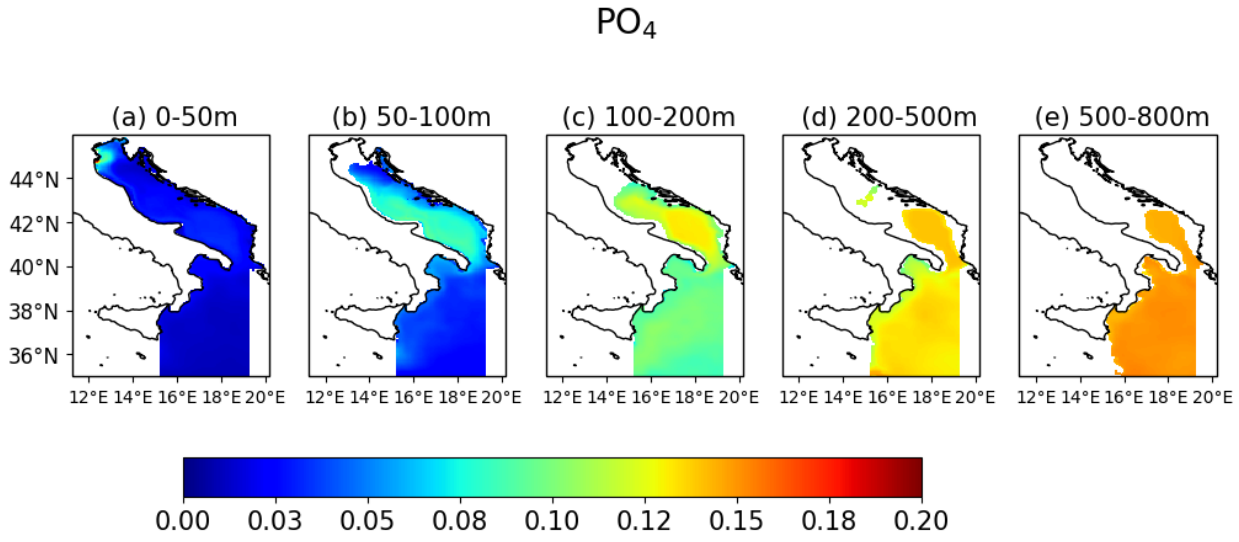

Figure 9 - Mean dissolved phosphate concentration (mmol/m3) for the period 1999-2018 in the layers between 0-50 m, 50-100 m, 100-200 m, 200-500 m and 500-800 m

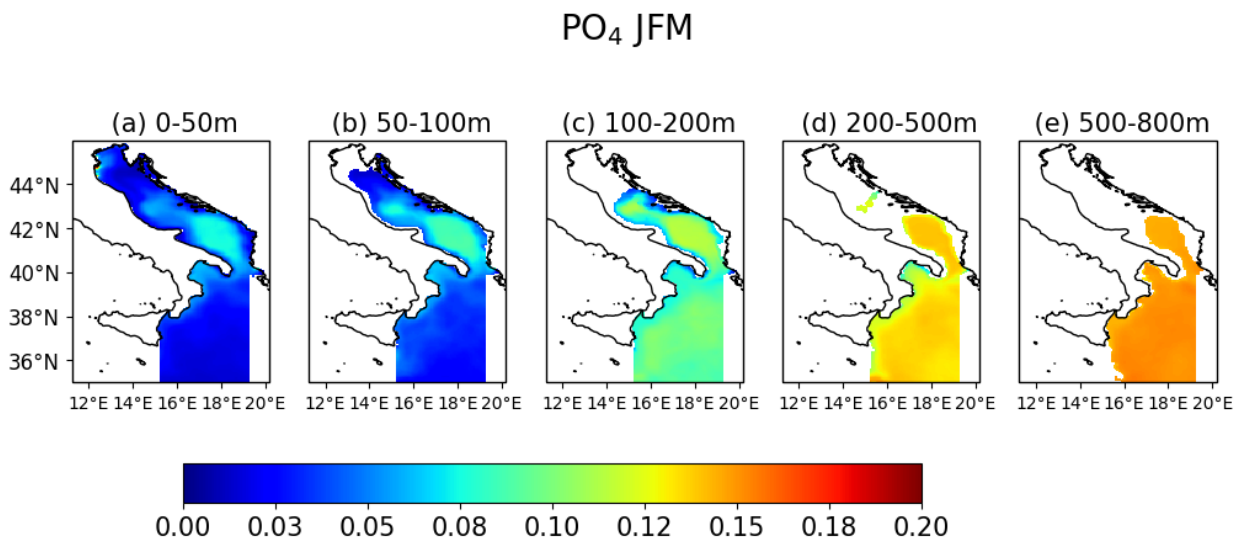

Figure 10 - Same as Fig. 9, but for JFM

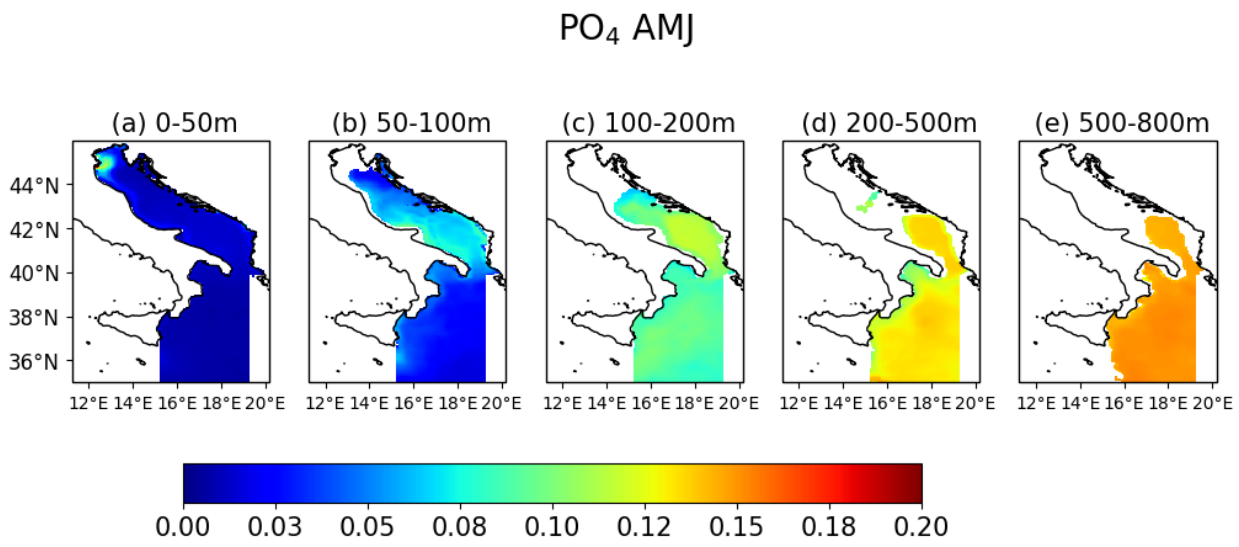

Figure 11 - Same as Fig. 10, but for AMJ

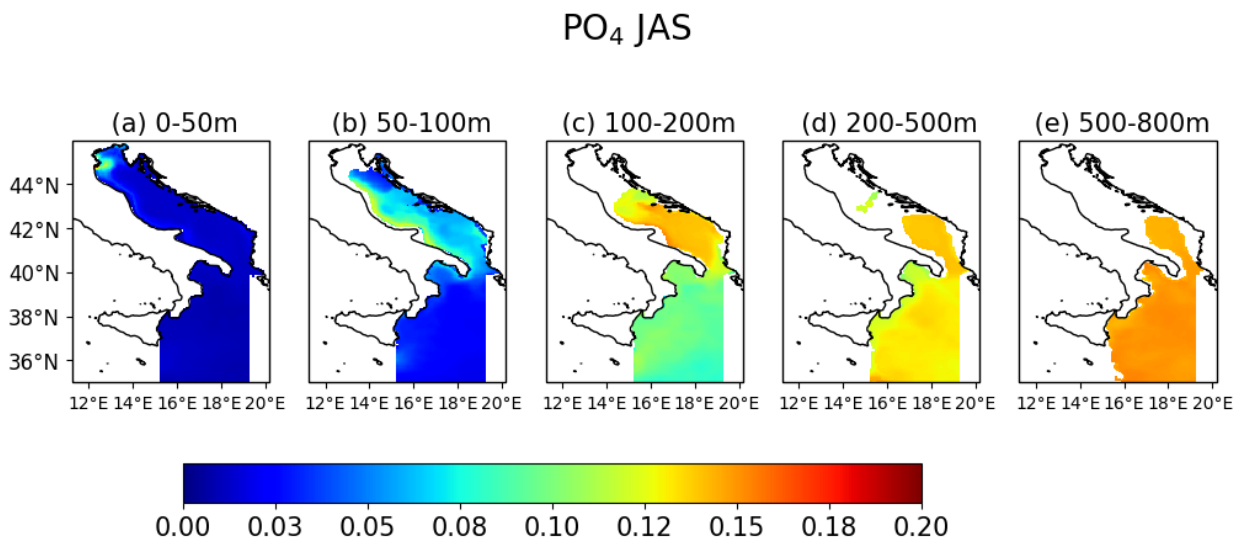

Figure 12 - Same as Fig. 11, but for JAS

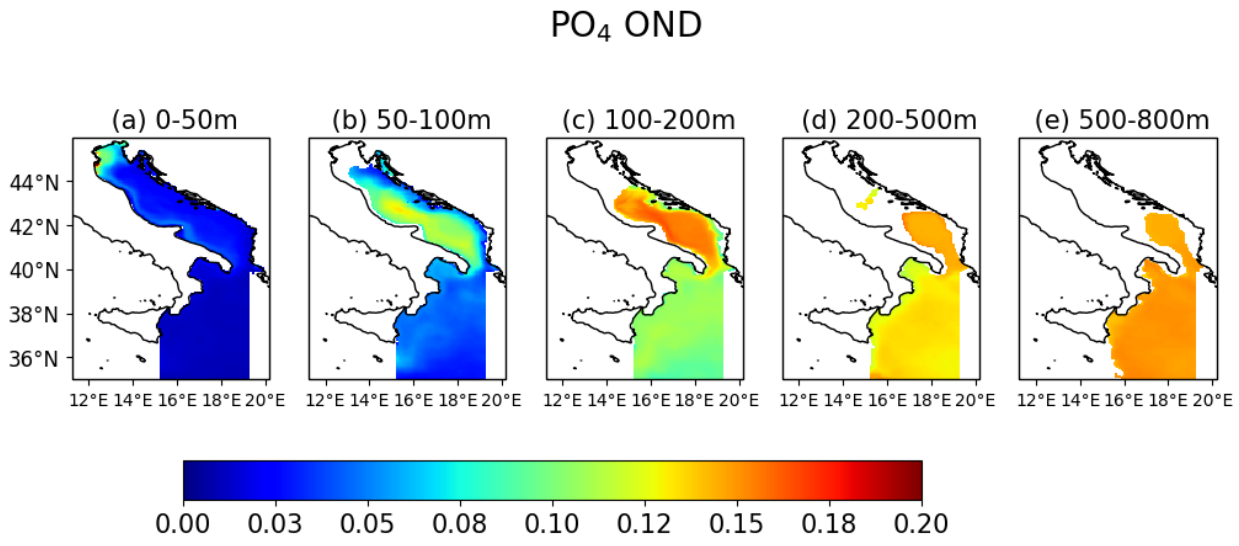

Figure 13 - Same as Fig. 12, but for OND

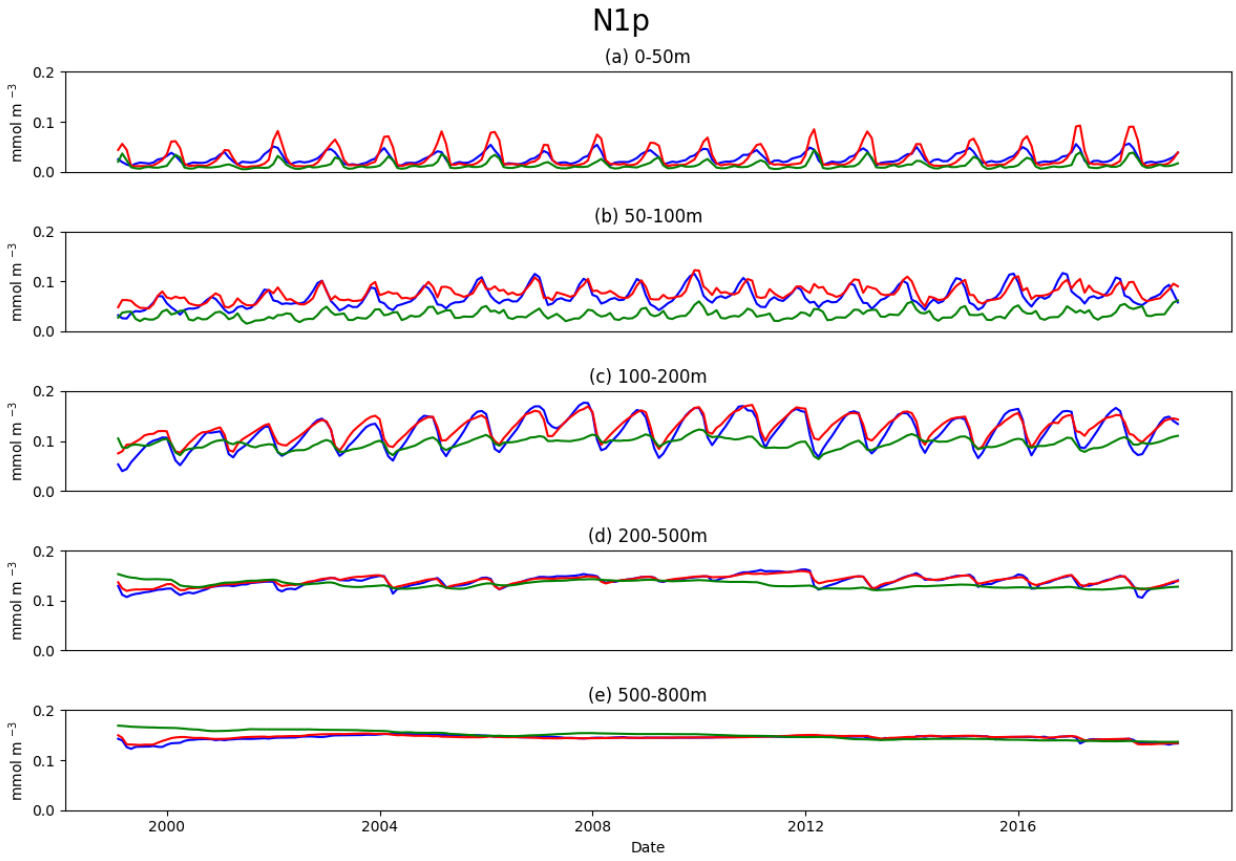

Figure 14 - Monthly timeseries of phosphate (mmol/m^3) in the three sub-areas of the Adriatic-Ionian domain (ADR1: blue, ADR2: red and IONIAN: green) in the period 1999-2018

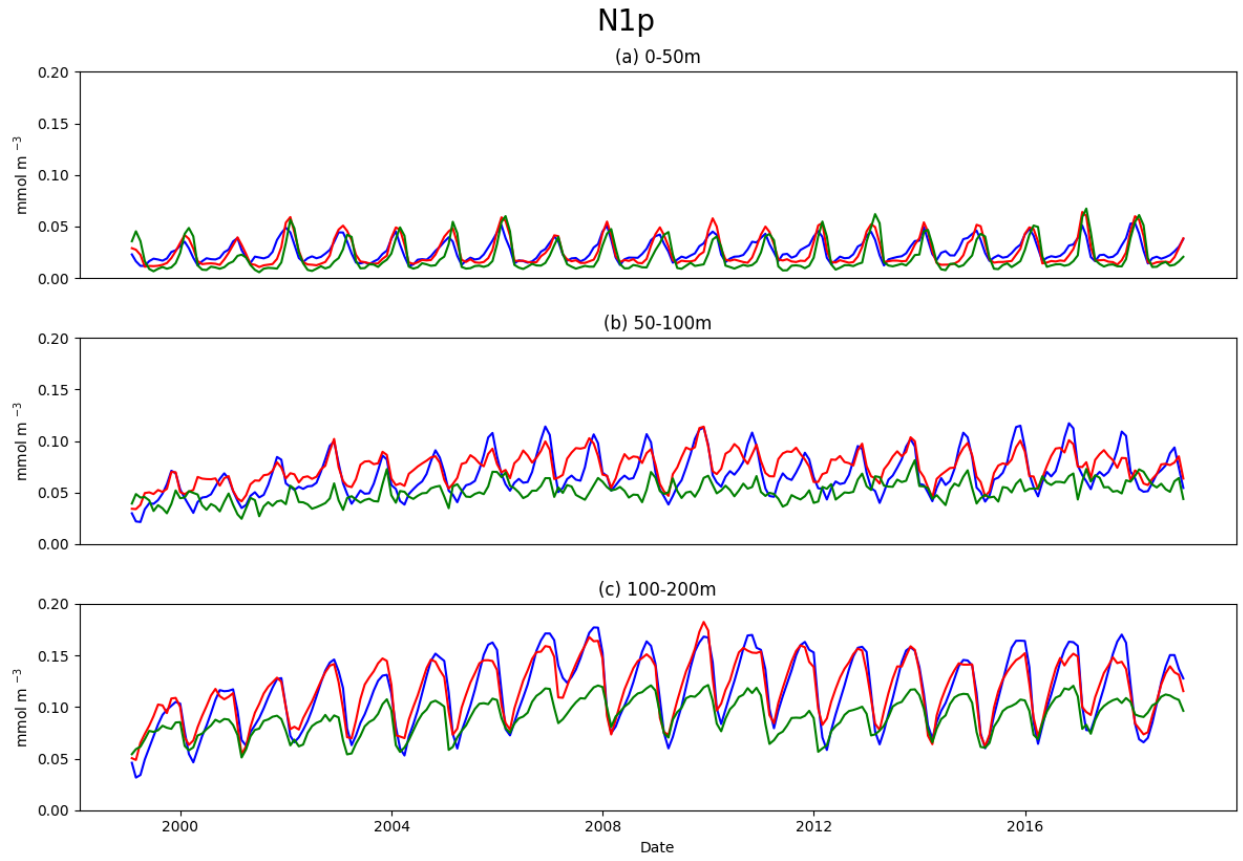

Figure 15 - Monthly timeseries of phosphate (mmol/m^3) in the inshore zone (depth less than 200 m) in the three sub-areas of the Adriatic-Ionian domain (ADR1: blue, ADR2: red and IONIAN: green) in the period 1999-2018

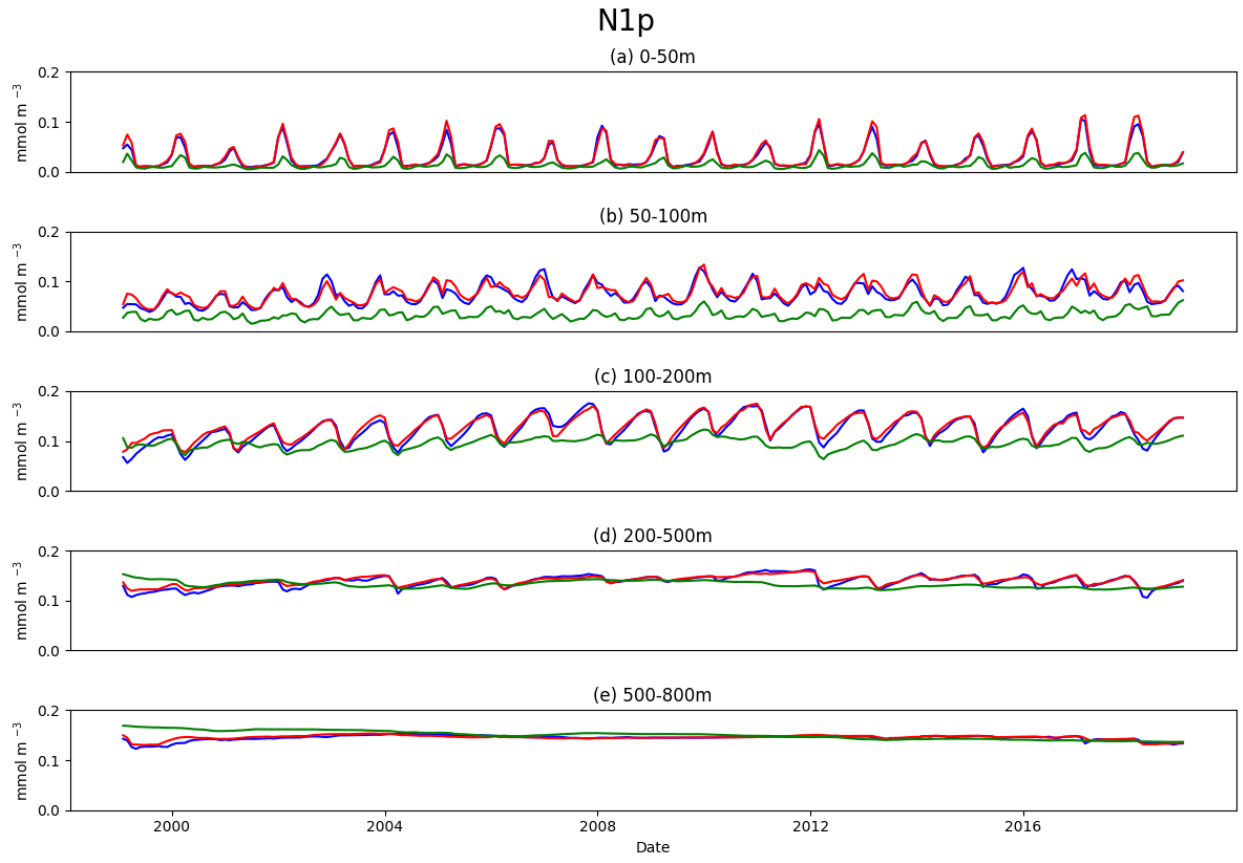

Figure 16 - Monthly timeseries of phosphate (mmol/m^3) in the offshore zone (deeper than 200 m) in the three sub-areas of the Adriatic-Ionian domain (ADR1: blue, ADR2: red and IONIAN: green) in the period 1999-2018

Phytoplankton biomass and chlorophyll

Fig. 17 and Fig. 25 shows the mean annual phytoplankton biomass (PHYC) and chlorophyll concentration computed at the five depths. The corresponding seasonal averages are shown Figs.18, 19, 20 and 21 and Figs. 26, 27, 28 and 29 for phytoplankton biomass and chlorophyll respectively. Both variables at the surface (0-50 m) show similar distribution, with higher concentrations in correspondence of the mouth of the Adriatic rivers due to the nutrient availability in those areas. From a seasonal point of view the

highest values are observed mainly in JFM and AMJ (Fig. 18-19 and Fig. 26-27) in correspondence of the peak of nutrient river discharges.

Significant signals for both variables are observed close to the Sicily coasts in JFM and AMJ due to upwelling phenomena that bring to the surface nutrient-rich deep water masses. Moving downwards between 50-100 m, the concentration of both variables is still relatively high in the southern Adriatic and northern Ionian in AMJ and JAS (Fig. 19-20 and Fig. 27-28): this is consistent with the position of the deep chlorophyll maximum (DCM) discussed in the literature. Below 100 m the concentration of phytoplankton fades, due to the limitation of short wave radiation.

Fig. 22, 23 and 24 and Fig. 30, 31 and 32 show the corresponding timeseries of three sub-areas (Fig. 22 and Fig. 30), and their inshore (Fig. 23 and Fig. 31) and offshore zones (Fig. 24 and Fig. 32). As shown before, phytoplankton biomass and chlorophyll tend to be higher at the surface in the Adriatic with respect to the Ionian. In the 50-100 m layer, the values between three sub-areas tend to be comparable, with a more marked annual cycle in the southern Adriatic due to the onset of DCM processes and winter light limitation. On the other hand, below 100 m, as already observed, the values tend to be lower with respect to those observed at the surface despite they are still higher in the Adriatic with respect to the Ionian Sea. In the inshore zones, values and behavior among the basins tend to be similar, with higher values in the surface layer.

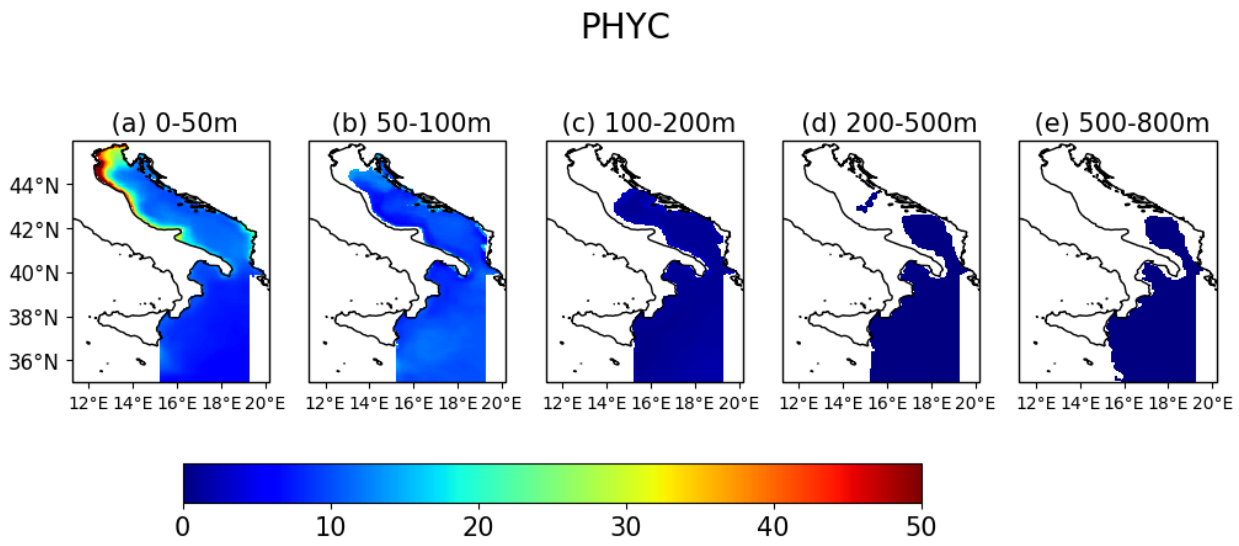

Figure 17 - Mean phytoplankton biomass (mgC/m^3) for the period 1999-2018 in the layers between 0-50 m, 50-100 m, 100-200 m,200-500 m and 500-800 m

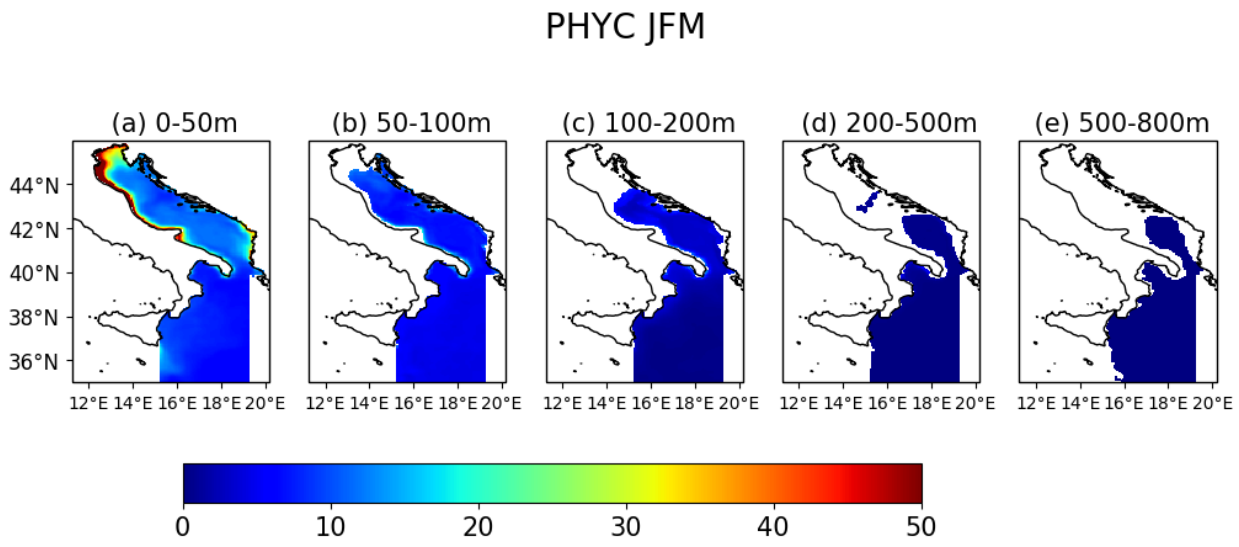

Figure 18 - Same as Fig. 17, for JFM

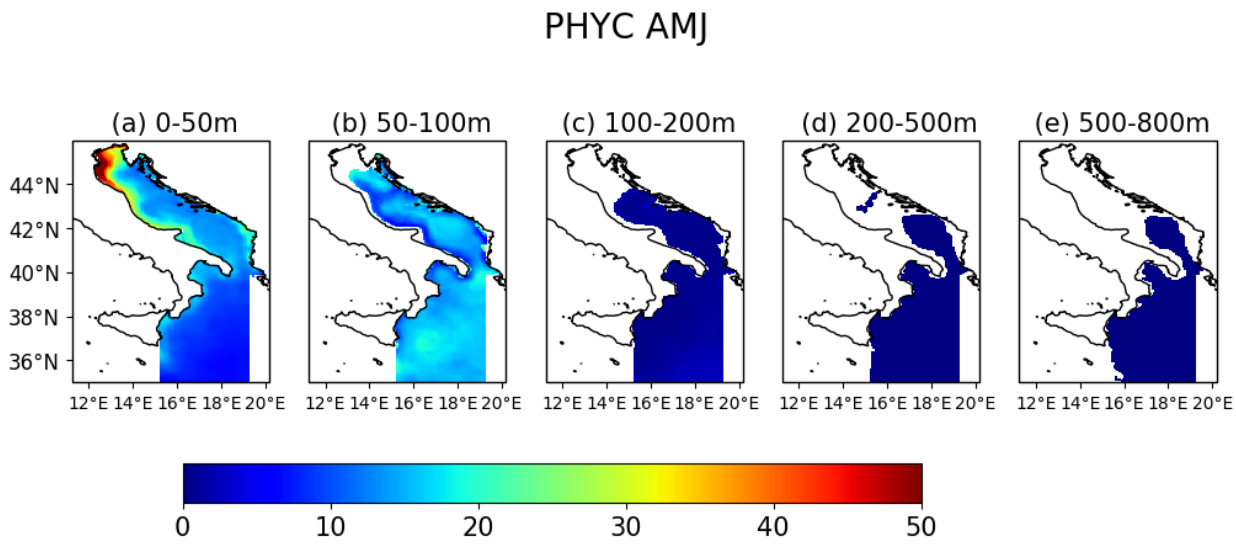

Figure 19 - Same as Fig. 18, for AMJ

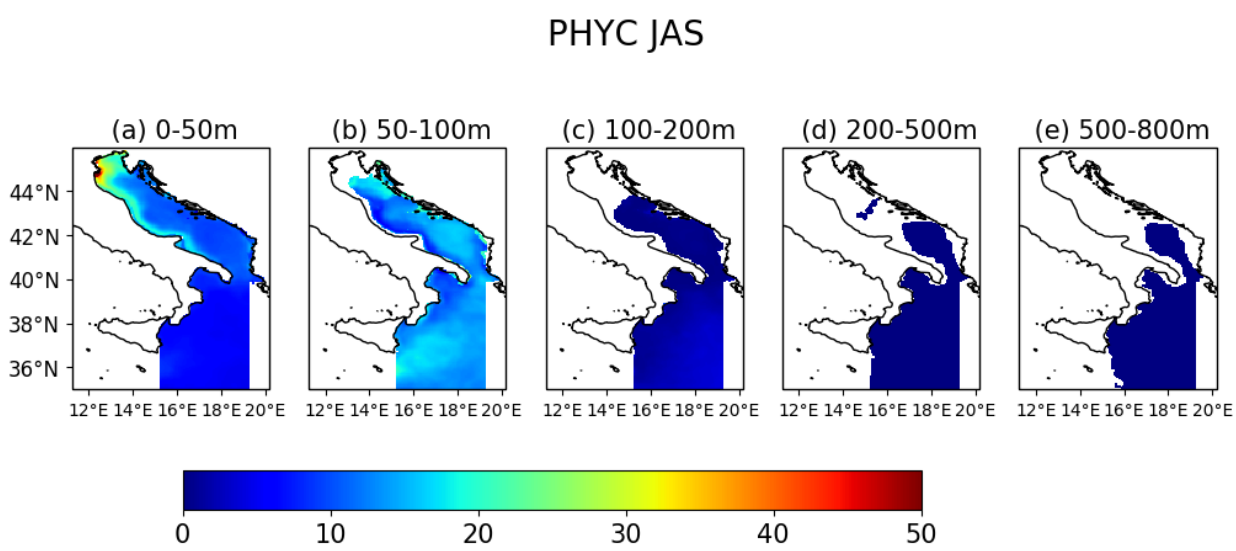

Figure 20 - Same as Fig. 19, for JAS

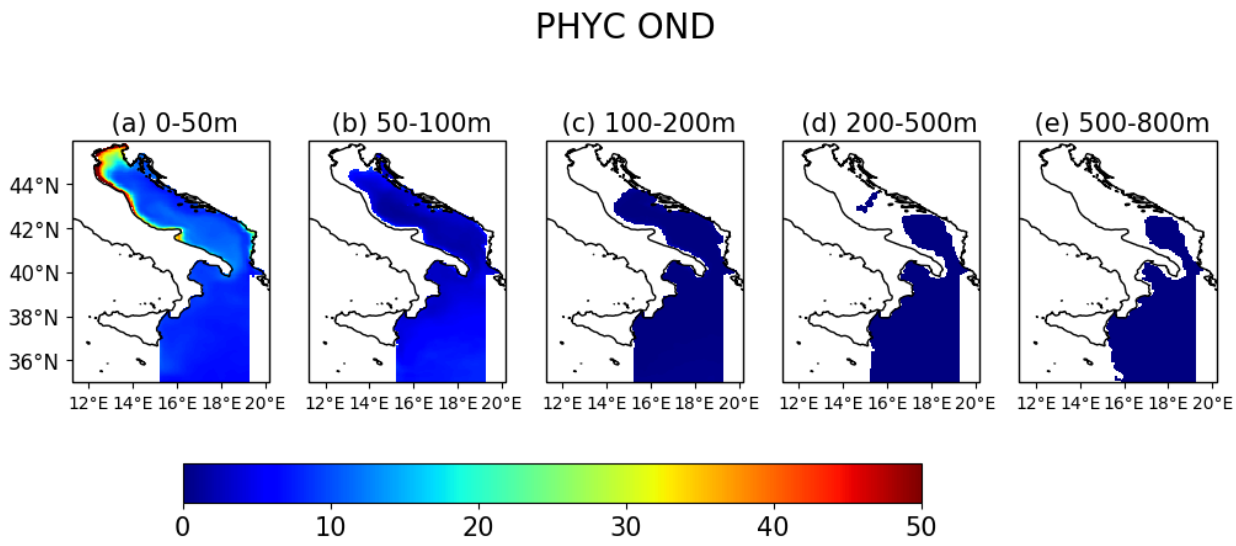

Figure 21 - Same as Fig. 20, for OND

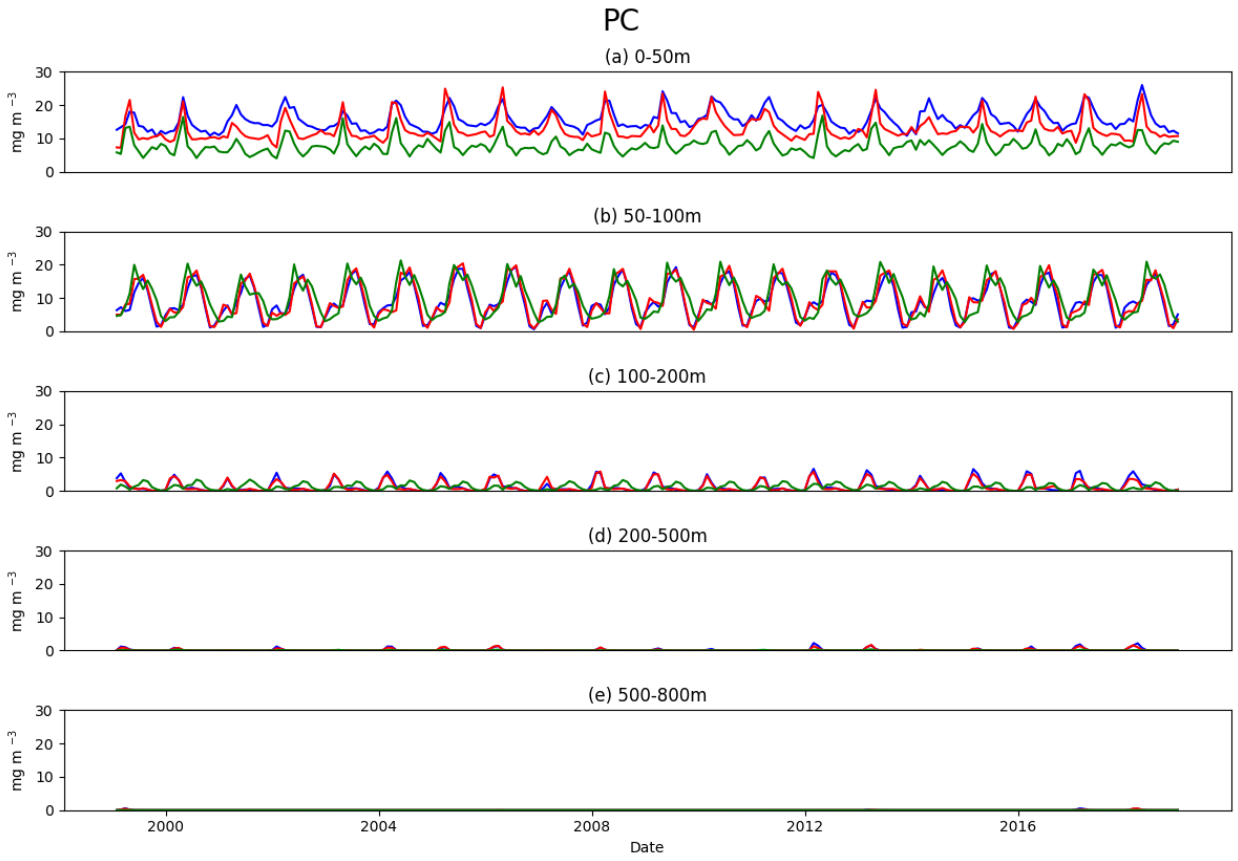

Figure 22 - Monthly timeseries of phytoplankton biomass (mgC/m^3) in the three sub-areas of the Adriatic-Ionian domain (ADR1: blue, ADR2: red and IONIAN: green) in the in the period 1999-2018

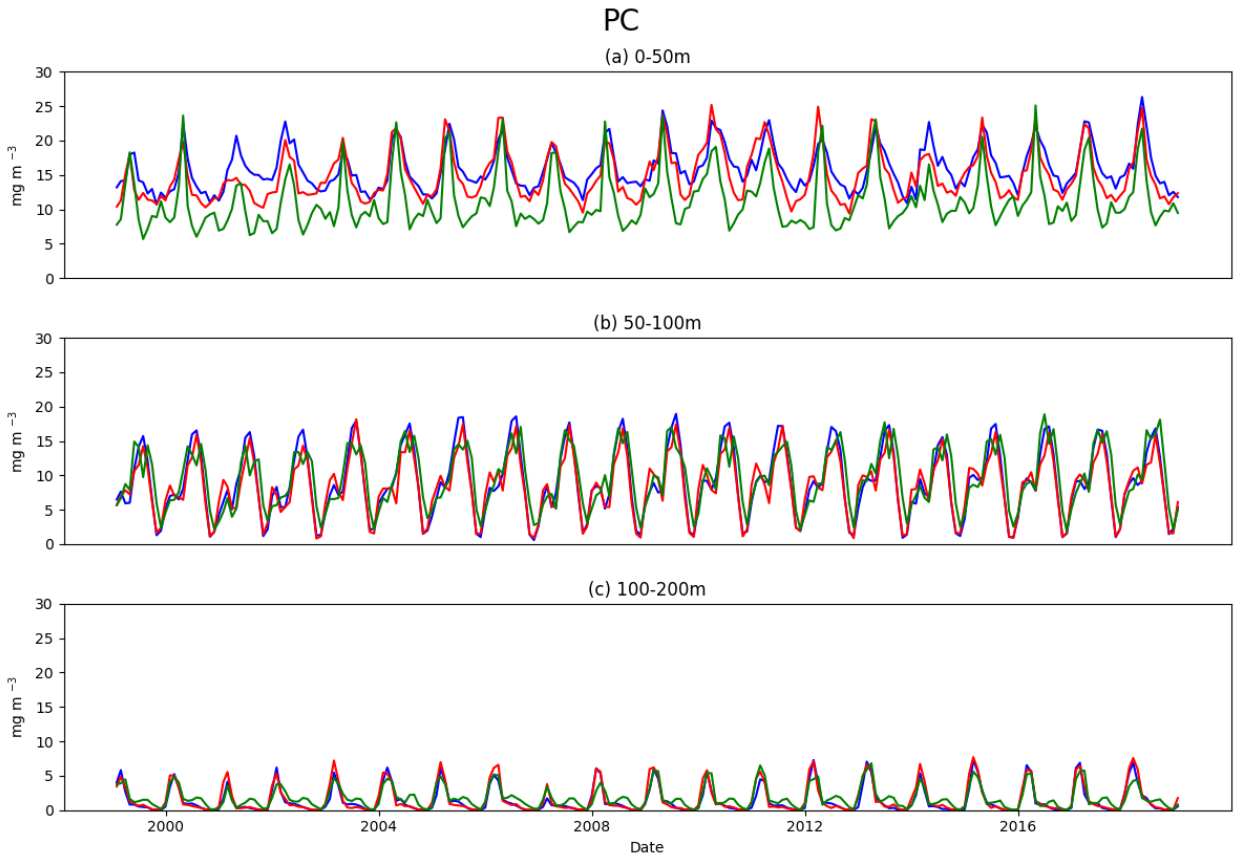

Figure 23 - Monthly timeseries of phytoplankton biomass (mgC/m^3) for inshore zones (depth less than 200 m) in the three sub-areas of the Adriatic-Ionian domain (ADR1: blue, ADR2: red and IONIAN: green) in the period 1999-2018

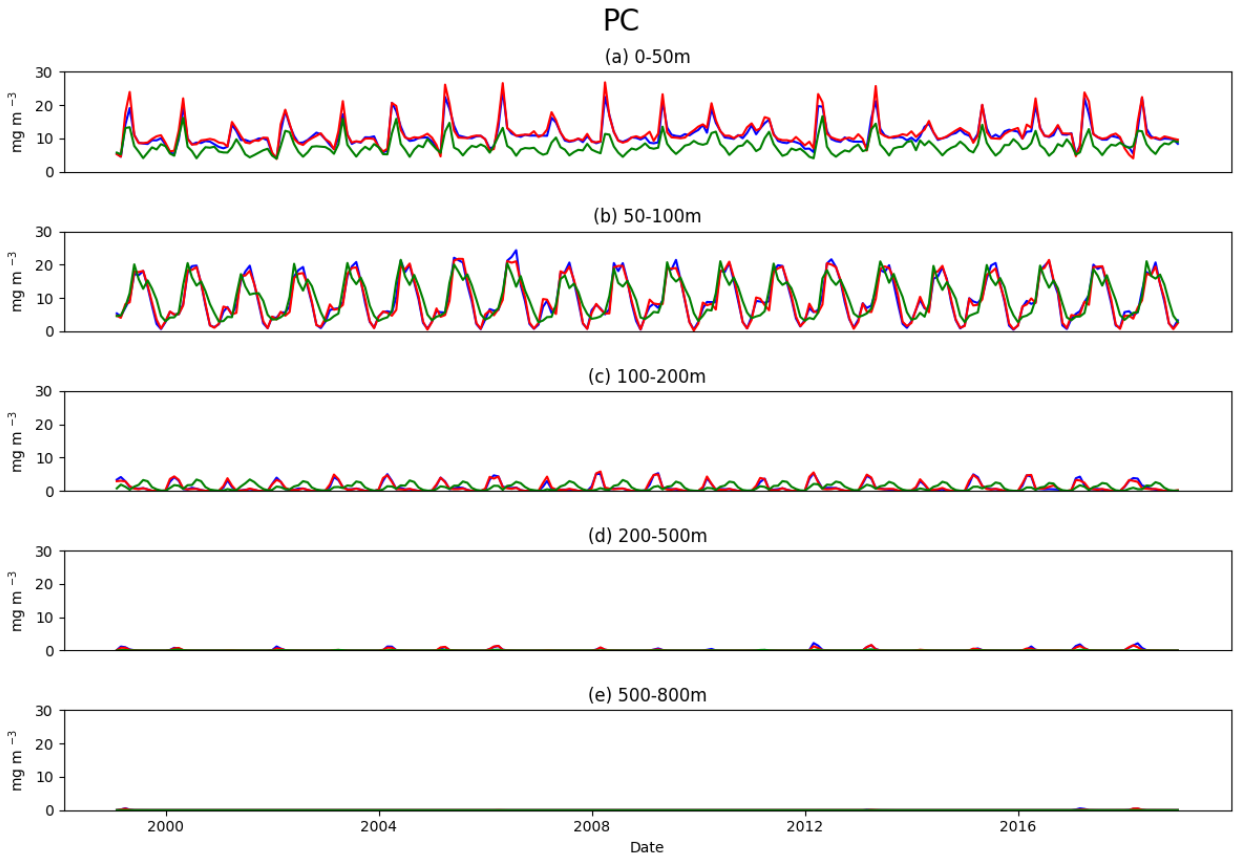

Figure 24 - Monthly timeseries of phytoplankton biomass (mg Carbon /m^3) for offshores zones (depth > 200 m) in the three sub-areas of the Adriatic-Ionian Sea domain (ADR1, blue, ADR2, red and IONIAN, green) in the in the period 1999-2018

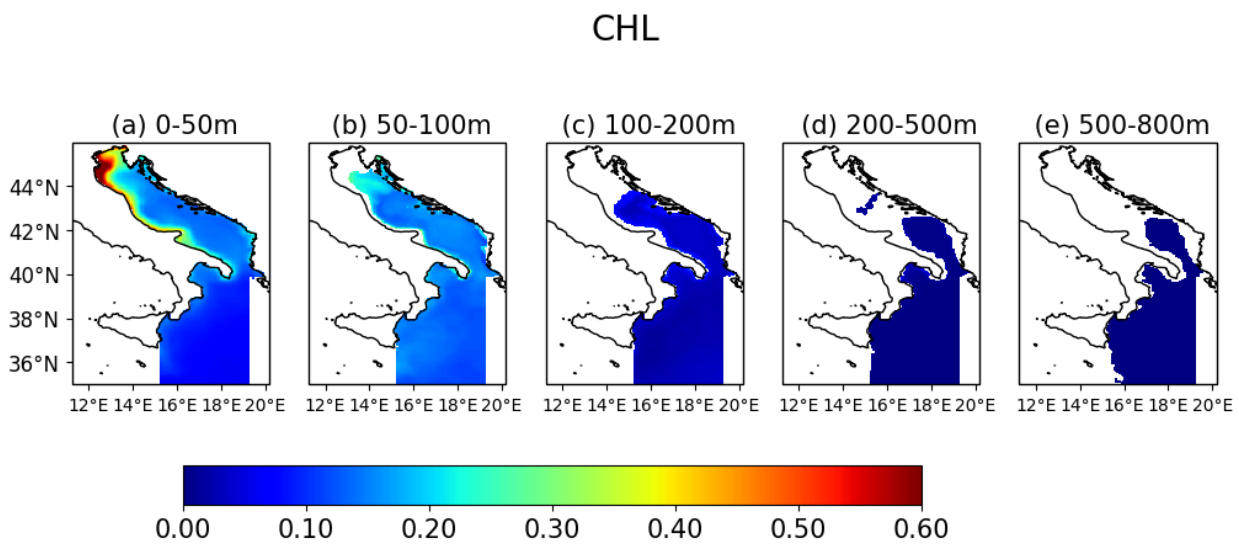

Figure 25 - Mean Chlorophyll-a concentration (mgChl-a/m^3) for the period 1999-2018 in the layer between 0-50 m, 50-100 m, 100-200 m, 200-500 m and 500-800 m

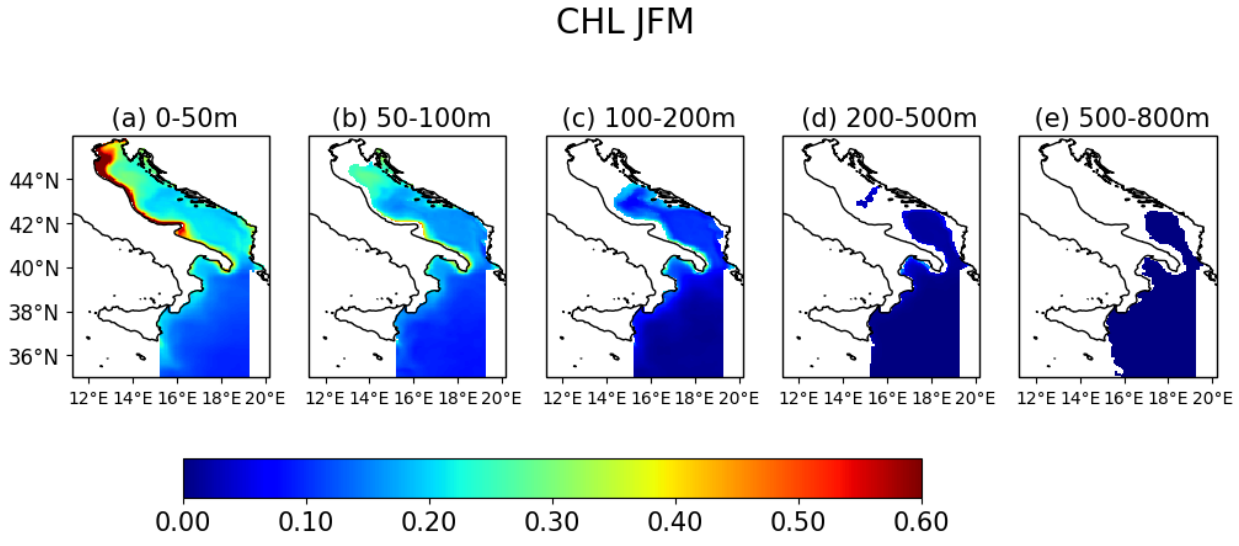

Figure 26 - Same as Fig. 25, but for JFM

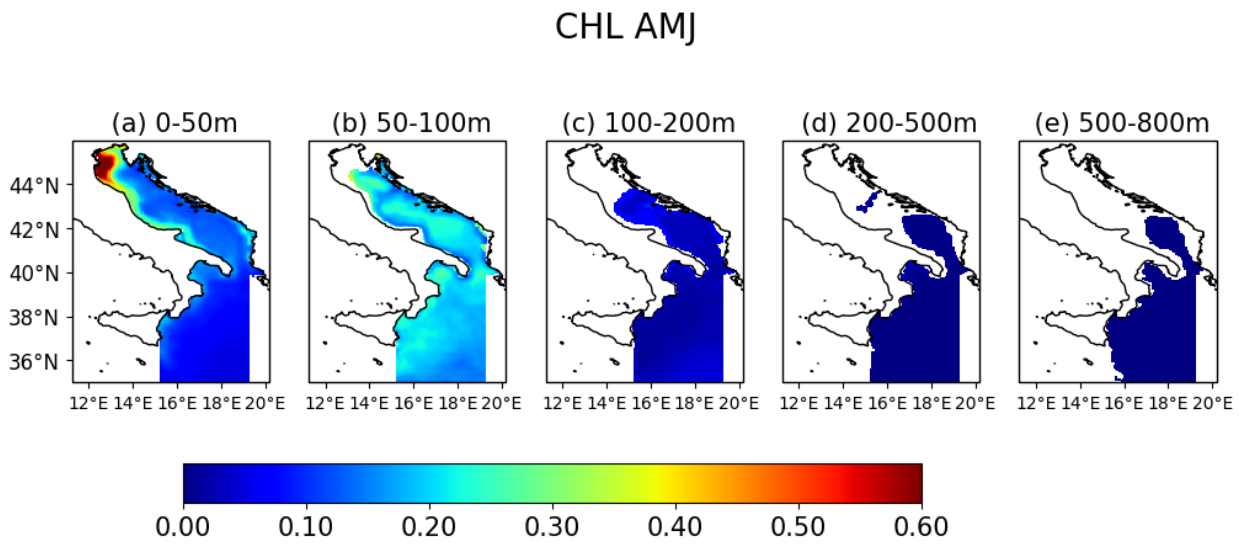

Figure 27 - Same as Fig. 26 for AMJ

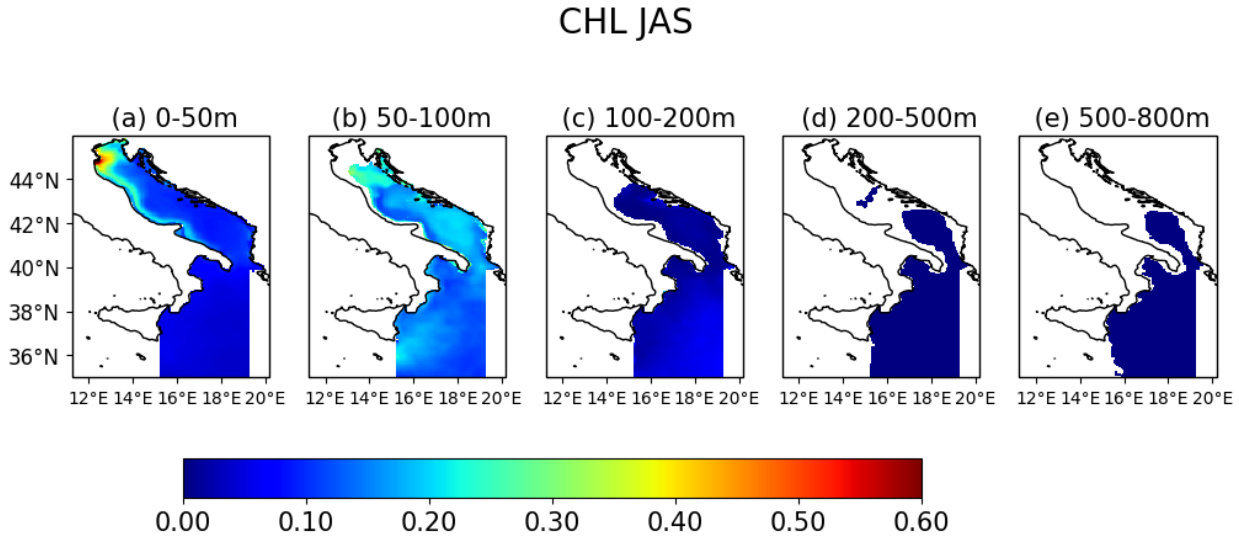

Figure 28 - Same as Fig. 27, for JAS

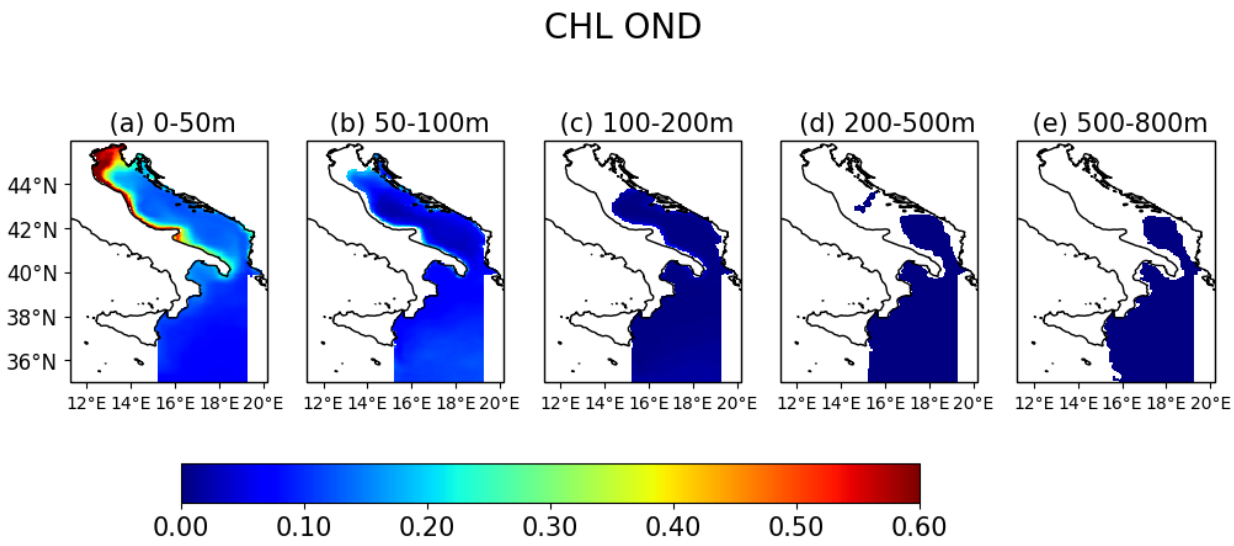

Figure 29 - Same as Fig. 28 for OND

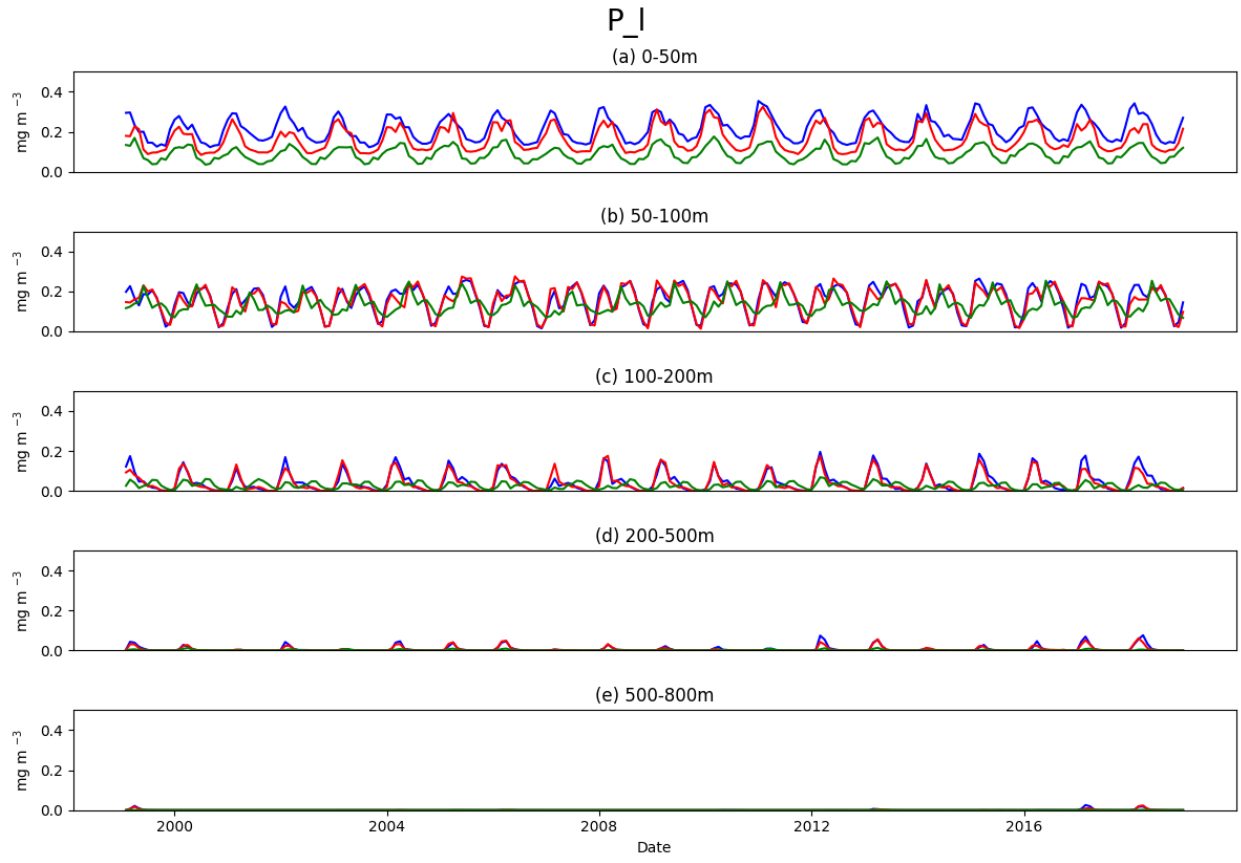

Figure 30 - Monthly timeseries of chlorophyll-a concentration (mgChl-a/m^3) in the three sub-areas of the Adriatic-Ionian domain (ADR1: blue, ADR2: red and IONIAN: green) in the period 1999-2018

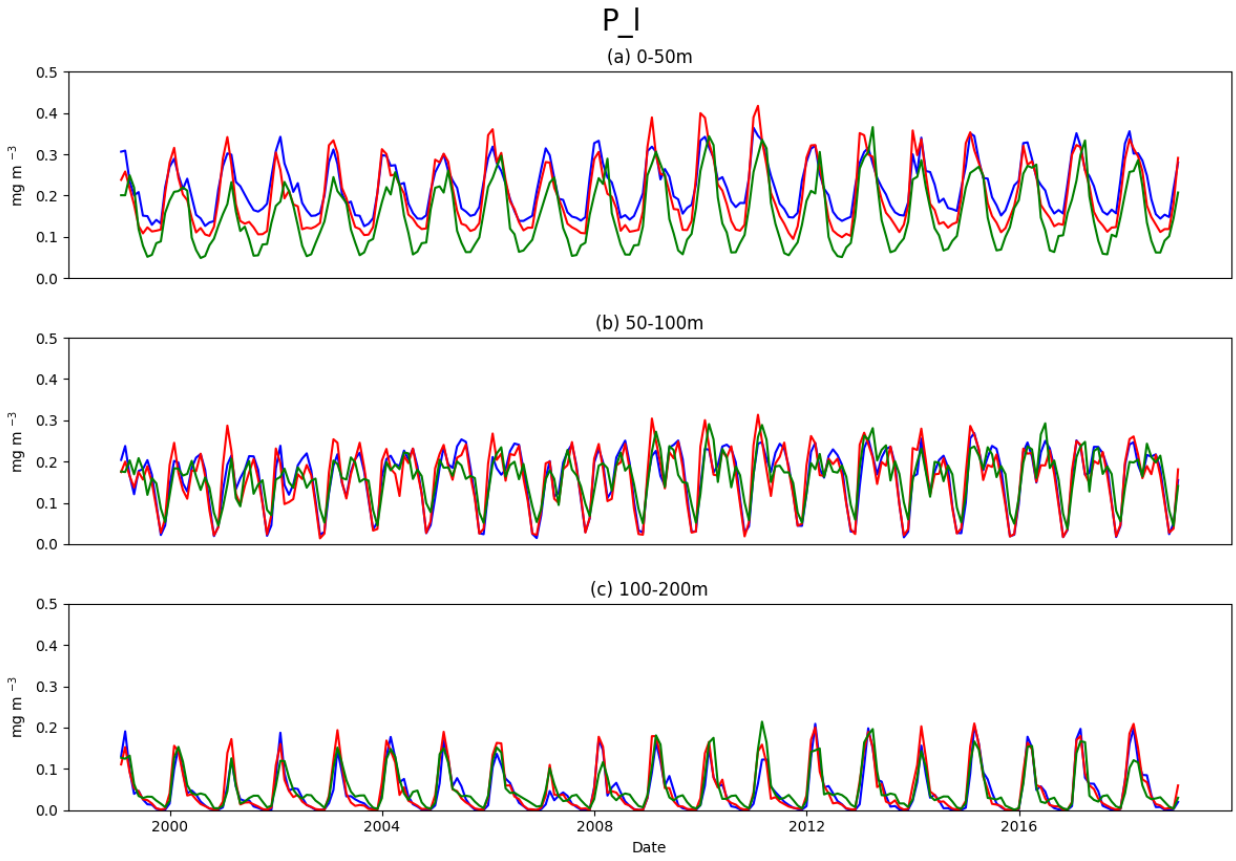

Figure 31 - Monthly timeseries of chlorophyll-a concentration (mgChl-a/m^3) for inshore zones (depth less than 200 m) in the three sub-areas of the Adriatic-Ionian domain (ADR1: blue, ADR2: red and IONIAN: green) in the period 1999-2018

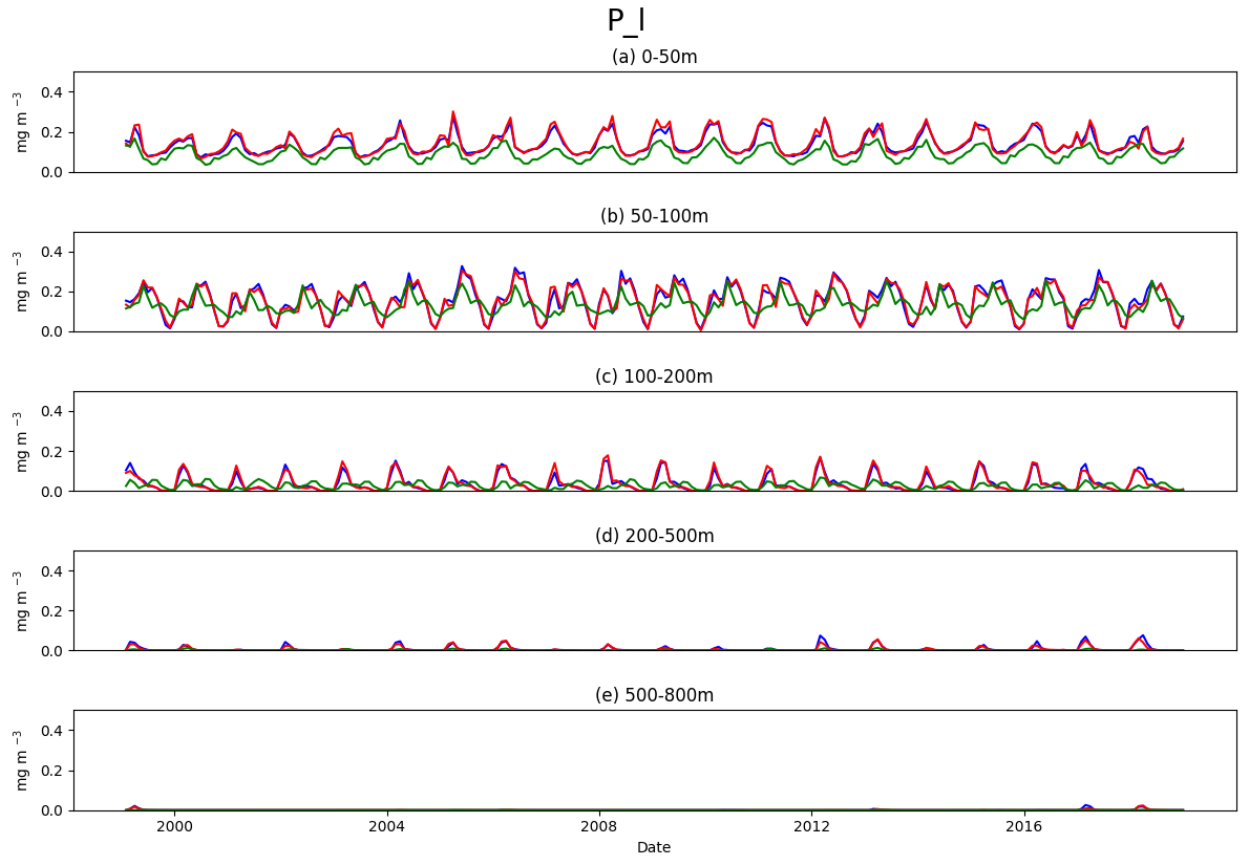

Figure 32 - Monthly timeseries of chlorophyll-a concentration (mgChl-a/m^3) for offshores zones (deeper than 200 m) in the three sub-areas of the Adriatic-Ionian domain (ADR1: blue, ADR2: red and IONIAN: green) in the period 1999-2018

Primary production

Fig. 33 shows the mean annual net primary production (NPP) computed at the five depths with the corresponding seasonal averages shown in Figs. 34, 35, 36 and 37. NPP is the difference between the carbon fixed during the photosynthesis and the one consumed during the respiration. NPP at the surface (0-50 m) shows a similar pattern to that observed for PHYC and Chl-a. In fact, higher values of concentration are simulated in correspondence of the mouth of the Adriatic rivers due higher nutrient availability in these

areas. Relatively higher values of PPN are observed mainly in JFM and AMJ (Fig. 34-35) following the seasonal cycle of nutrient river discharges and light limitation. As observed for the chlorophyll-a and phytoplankton biomass, marked signals are simulated close to the Sicily coastlines due to the presence of the upwelling phenomena occurring in JFM and AMJ. When moving downwards, NPP decreases or even it becomes negative due to the prevalence of the respiration process with respect to photosynthesis. Figs. 38, 39 and 40 show the corresponding time series of three sub-areas (Fig. 38) and their inshore (Fig. 39) and offshore zones (Fig. 40). NPP is higher in the Adriatic with respect to the Ionian at surface and in the inshore areas, mirroring the trophic gradient shown for the limiting nutrient (PO_4). NPP tends to become lower and negative below 100 m due to the light limitation and the prevalence of respiration over photosynthesis.

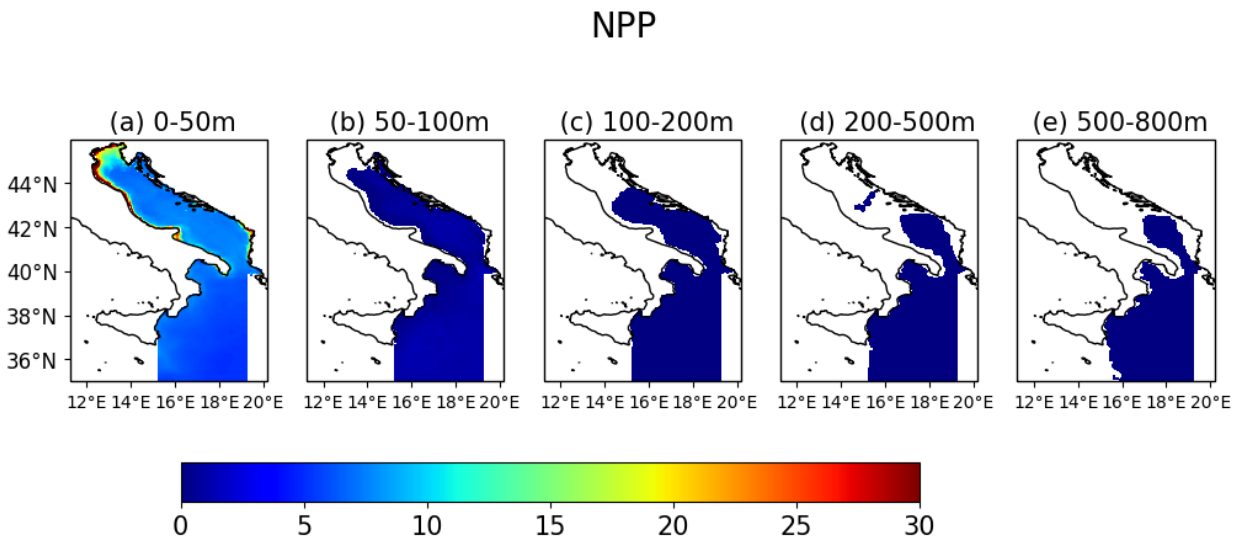

Figure 33 - Mean NPP (mgC/m^3/day) for the period 1999-2018 in the layer between 0-50 m, 50-100 m, 100-200 m, 200-500 m and 500-800 m

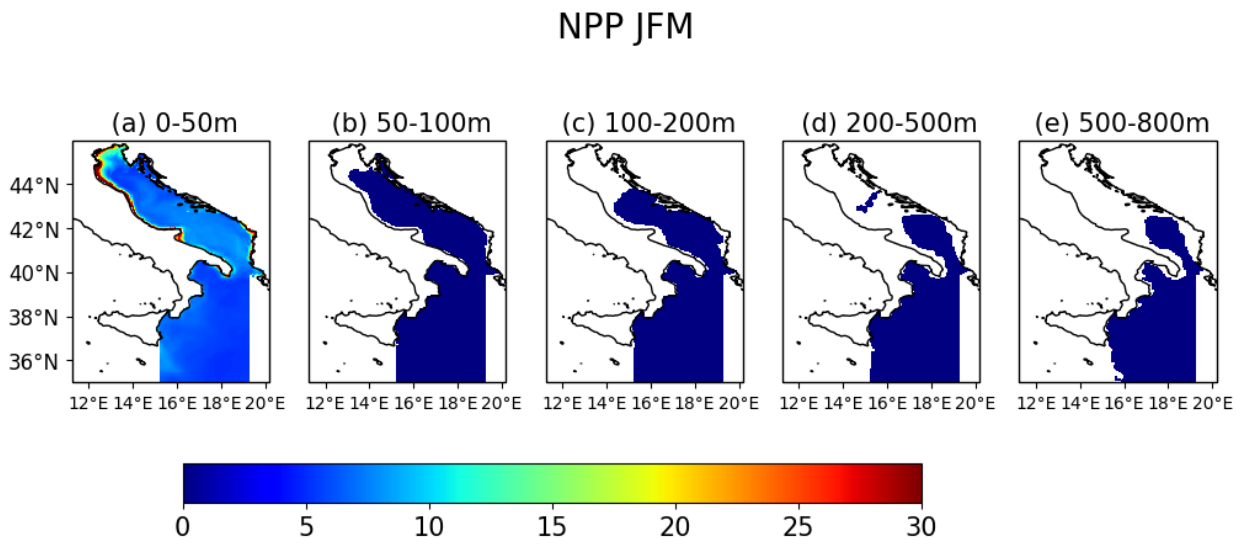

Figure 34 - Same as Fig. 33, but for JFM

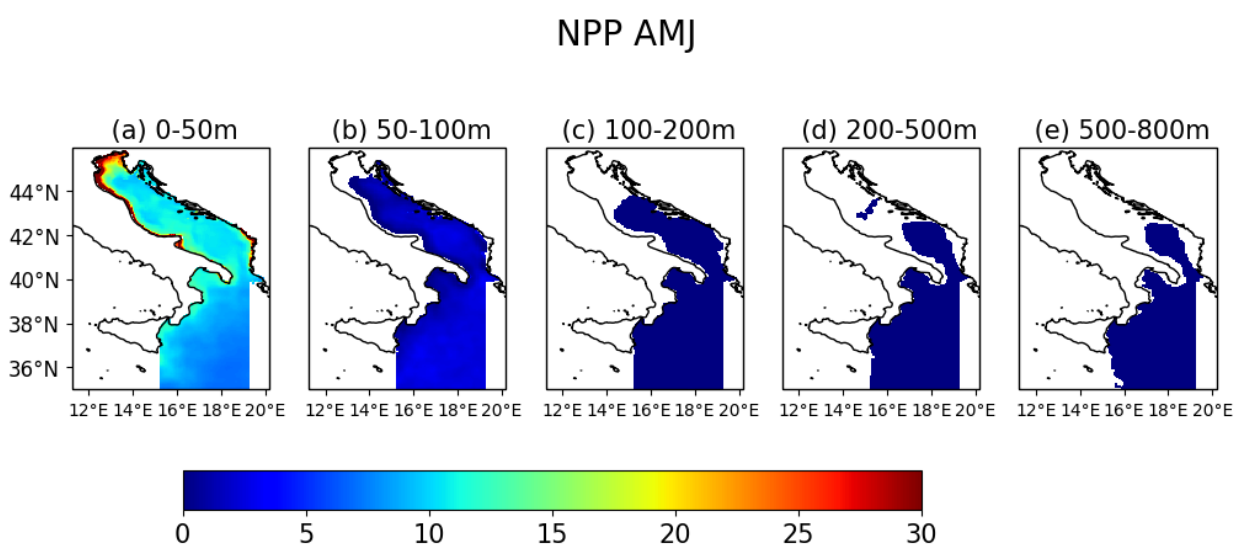

Figure 35 - Same as Fig. 34, but for AMJ

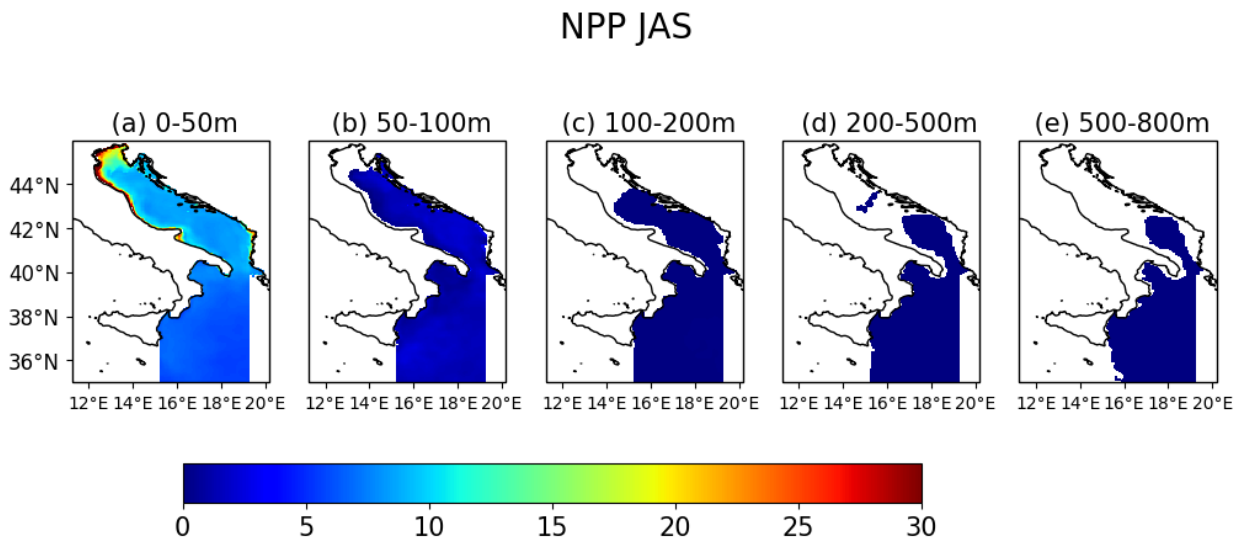

Figure 36 - Same as Fig. 35, for JAS

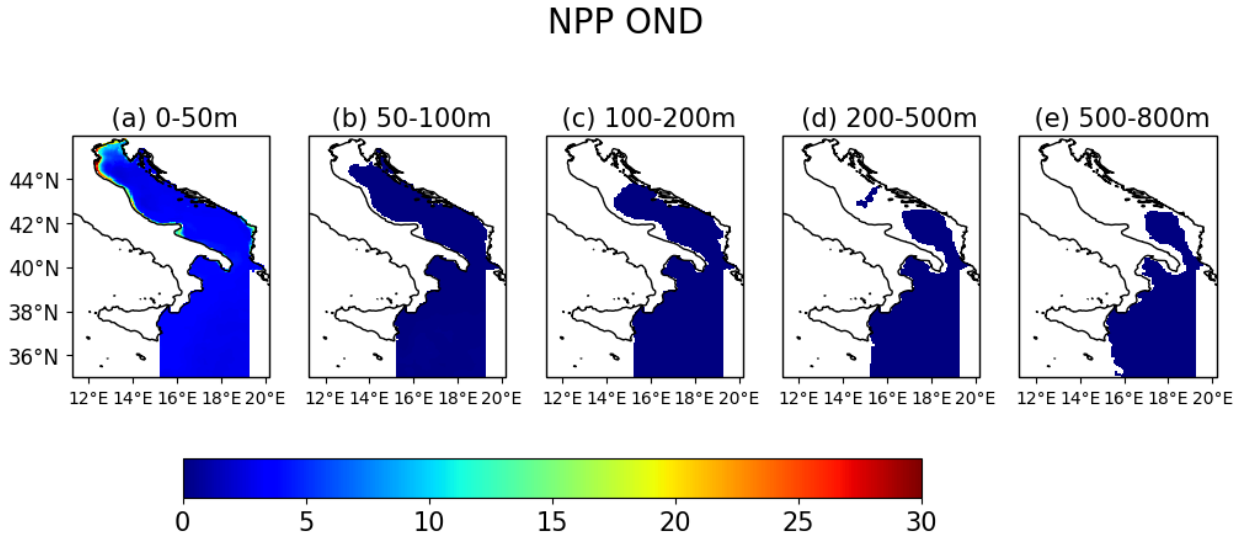

Figure 37 - Same as Fig. 36, for OND

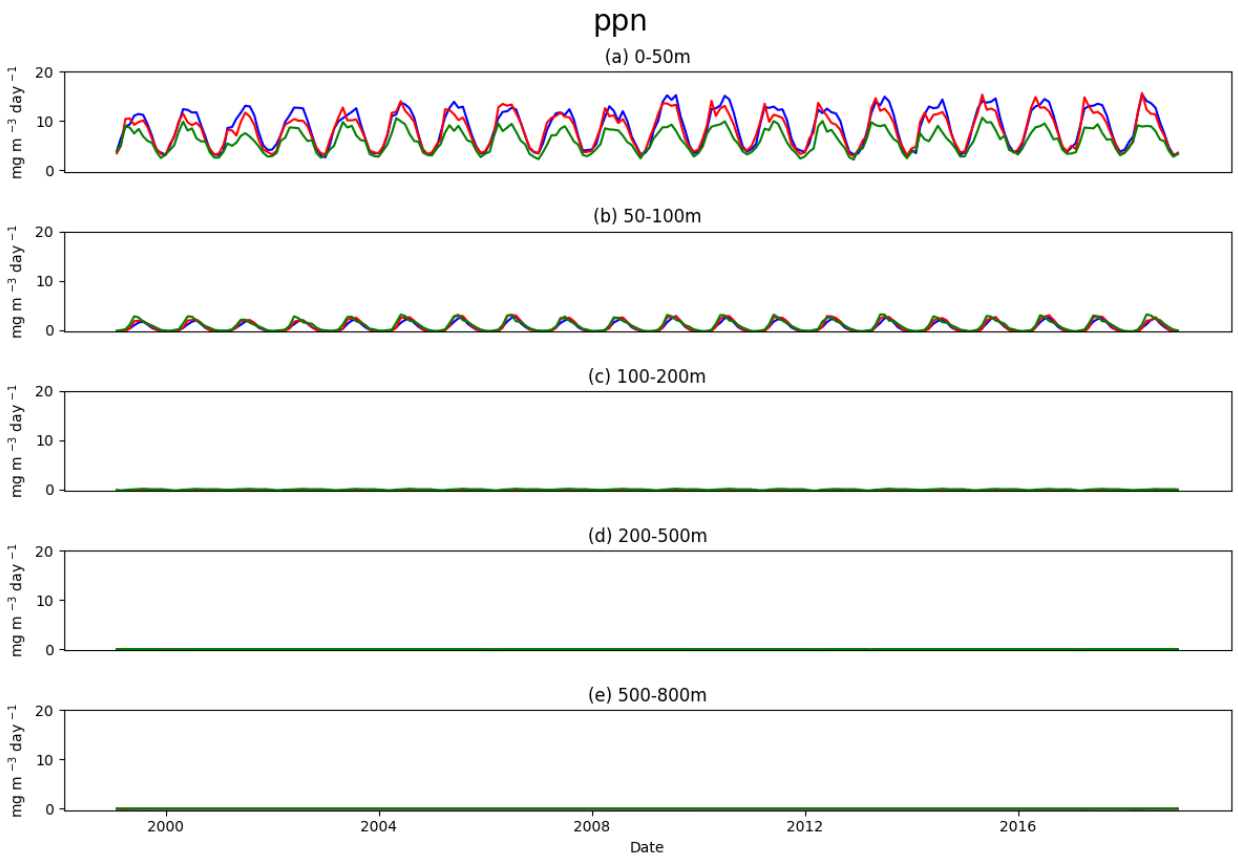

Figure 38 - Monthly timeseries of net primary production (mgC/m^3/day) in the three sub-areas of the Adriatic-Ionian domain (ADR1: blue, ADR2: red and IONIAN: green) in the period 1999-2018

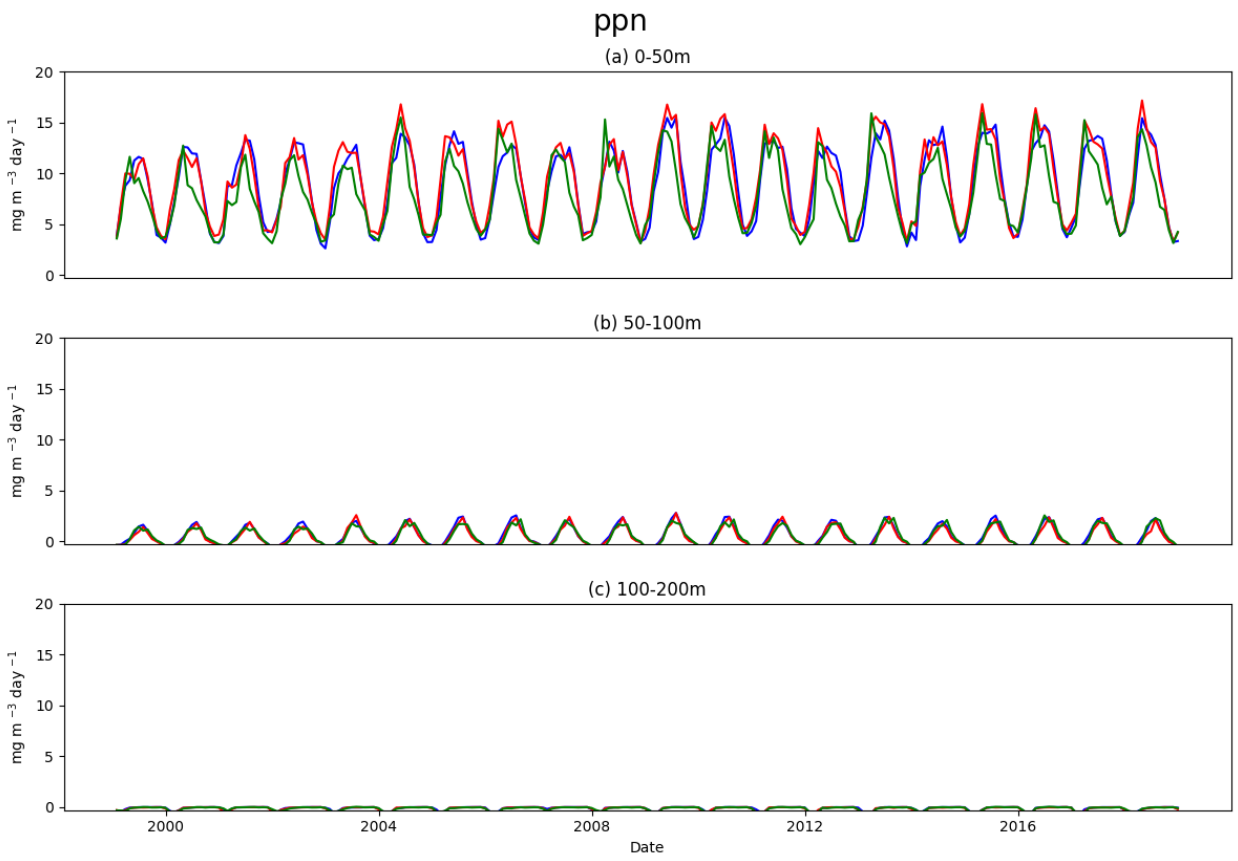

Figure 39 - Monthly timeseries of net primary production (mgC/m^3/day) in the inshore (depth less than 200 m) zones of three sub-areas of the Adriatic-Ionian domain (ADR1: blue, ADR2: red and IONIAN: green) in the period 1999-2018

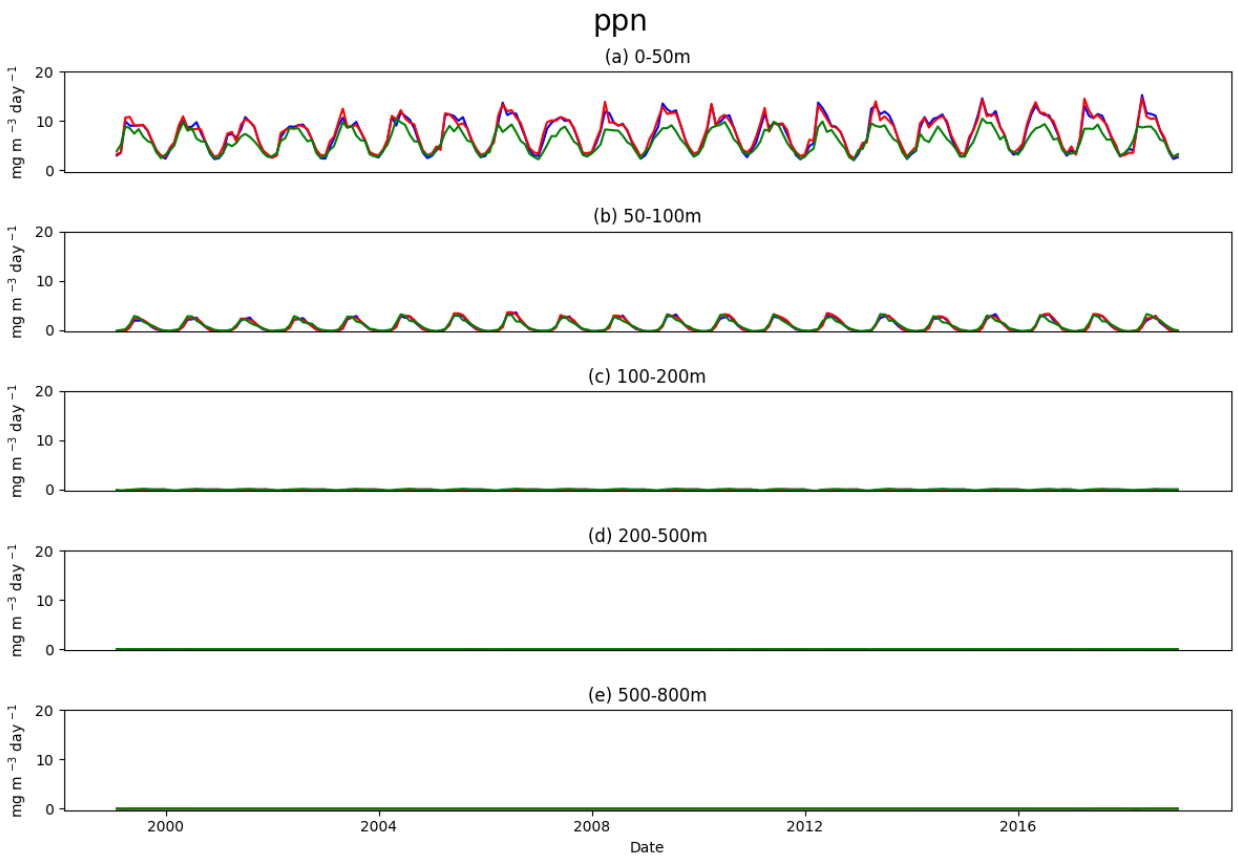

Figure 40 - Monthly timeseries of net primary production (mgC/m^3/day) in the offshore (deeper than 200 m) zones of three sub-areas of the Adriatic-Ionian domain (ADR1: blue, ADR2: red and IONIAN: green) in the period 1999-2018

Dissolved oxygen and bottom oxygen

Fig. 41 shows the mean annual dissolved oxygen computed at the five depths, while the corresponding seasonal averages are shown in Figs. 42, 43, 44 and 45. Adriatic (mainly its northern part) is characterized by higher values of dissolved oxygen with respect to the Ionian.

The highest values of dissolved oxygen are observed in JFM, the lowest in JAS, following the seasonal cycle of the solubility. Highest values are observed in northern Adriatic Sea,

with a minimum of dissolved oxygen in correspondence of the Po river mouth due to the effect of dilution operated by the river discharge. Moving downwards along the water column, dissolved oxygen concentration generally decreases. The southern Adriatic is still characterized throughout the year by relatively higher values of oxygen due to the mixing of the surface water (rich in oxygen) with the layers below. Figs. 46, 47 and 48 show the corresponding time series of the three sub-areas (Fig. 46), and their inshore (Fig. 47) and offshore zones (Fig. 48). Dissolved oxygen concentration is higher in the Adriatic with respect to the Ionian. In the Adriatic basin, the northern area is richer in oxygen than the southern one, even if the behavior between the two areas is similar. In the in-shore areas the behavior and values among the basins are very similar (Fig. 47).

When looking at the oxygen concentration at the bottom of the water column (Fig. 49), the northern Adriatic shows higher concentrations with respect to the southern Adriatic and Ionian Seas. Coastal areas have higher values than offshore. These patterns are associated with the depth of the water column. Close to northern Adriatic river mouths, the fresh water dilution effect (and secondarily the excess of respiration over production at the bottom) prevails on the solubility and air-sea fluxes. Further, the highest bottom oxygen values are observed in the eastern part of the northern Adriatic Sea: probably they are associated with the cold and rich-in-oxygen deep water production during winter.

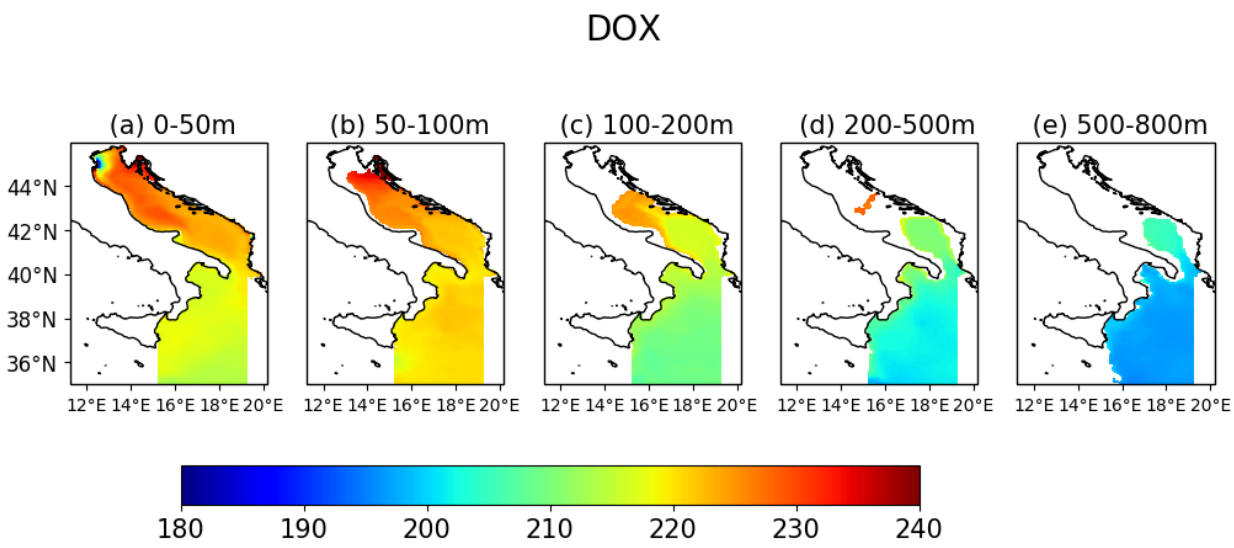

Figure 41 - Mean dissolved oxygen (mmol/m^3) for the period 1999-2018 in the layers between 0-50 m, 50-100 m, 100-200 m, 200-500 m and 500-800 m

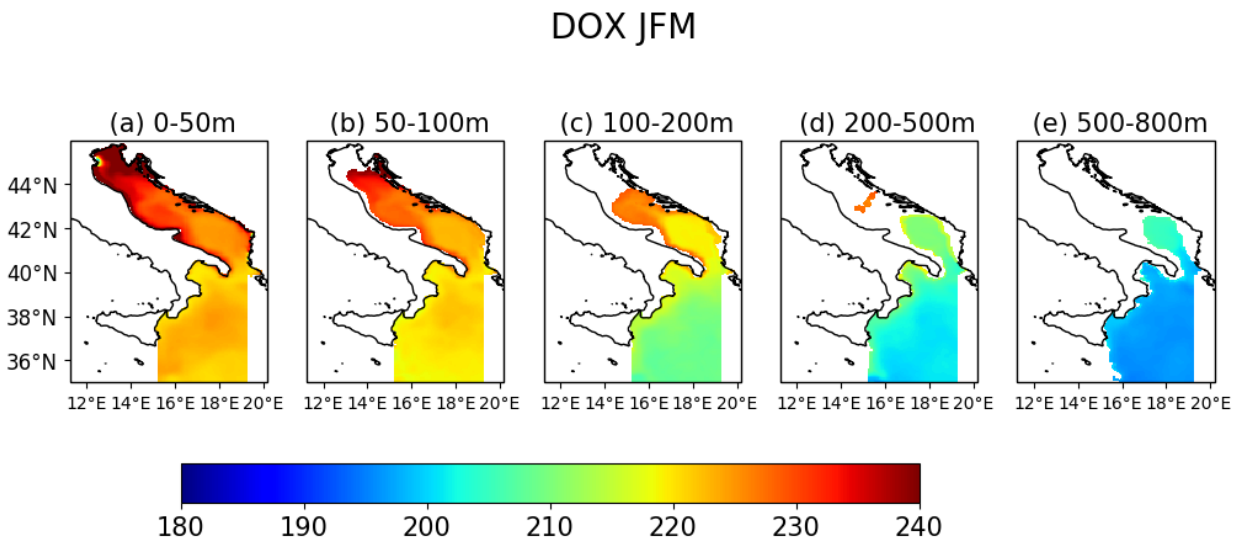

Figure 42 - Same as Fig. 41, for JFM

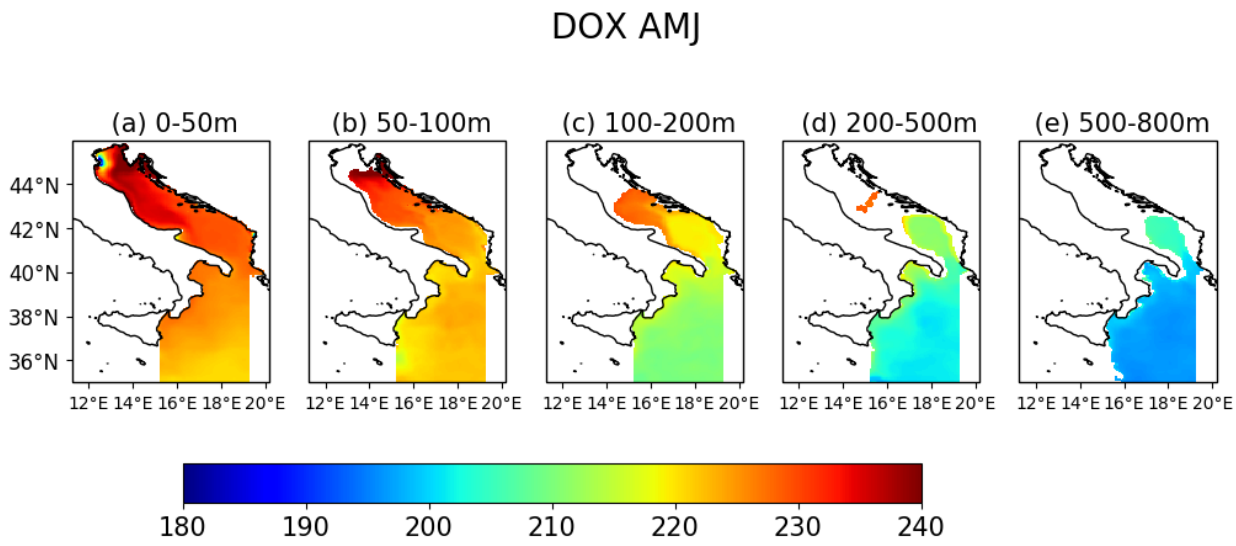

Figure 43 - Same as Fig. 42, for AMJ

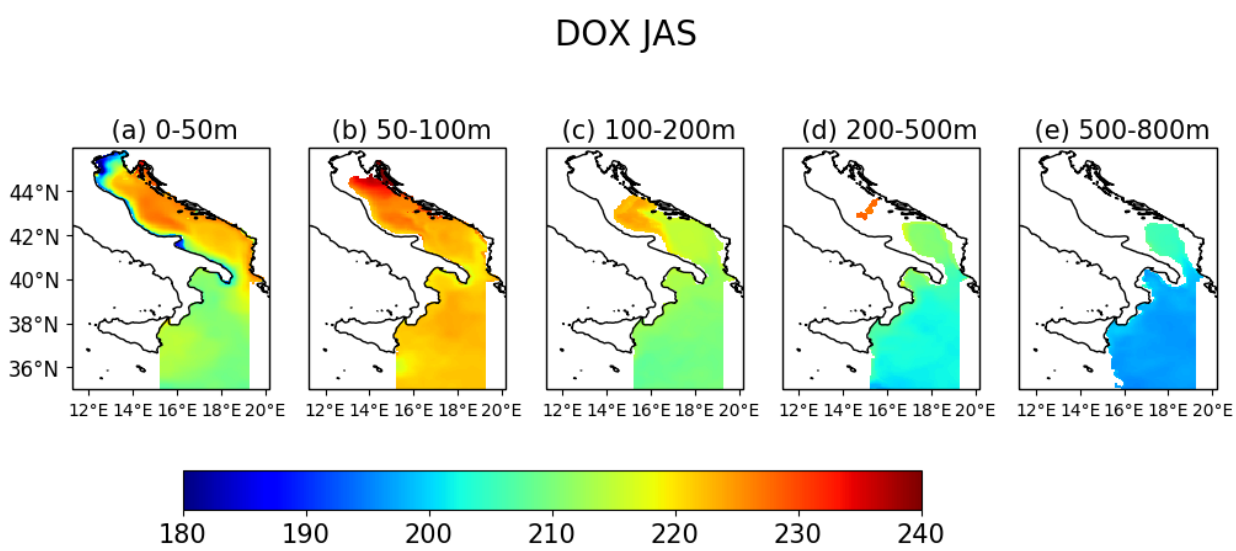

Figure 44 - Same as Fig. 43, for JAS

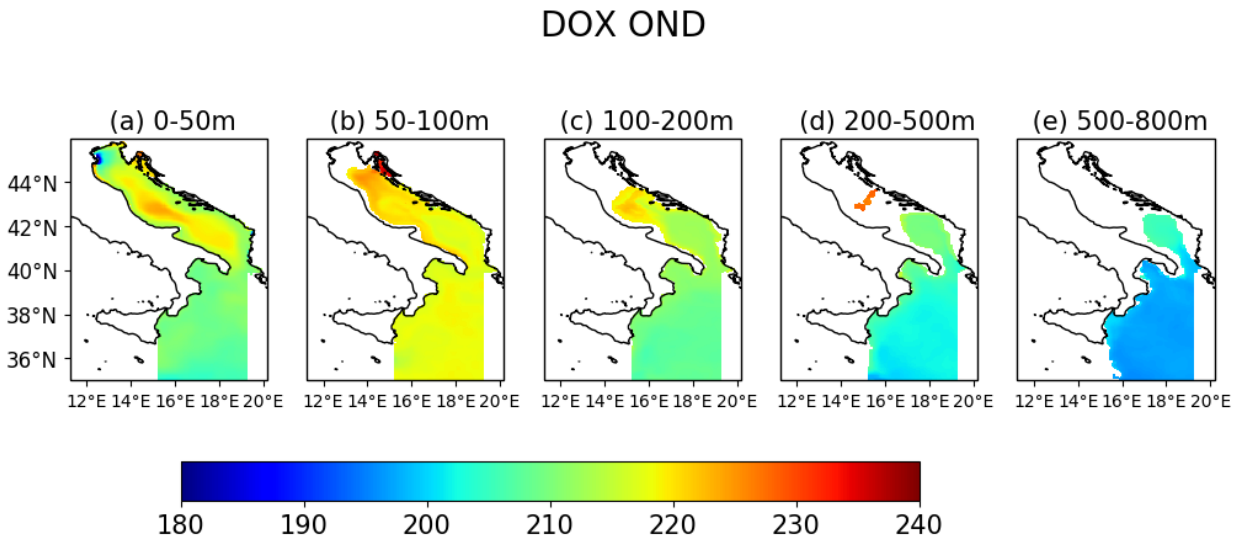

Figure 45 - Same as Fig. 44, for OND

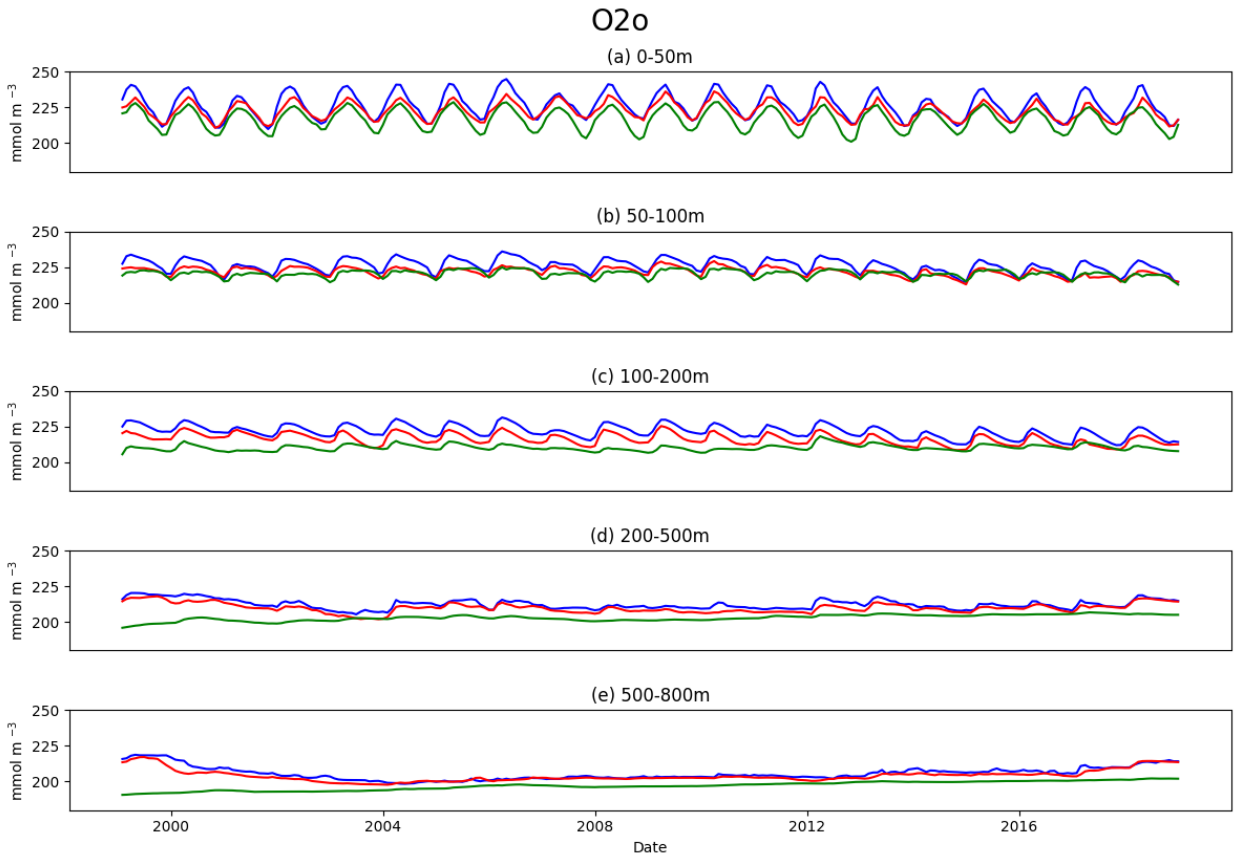

Figure 46 - Monthly timeseries of dissolved oxygen (mmol/m^3) in the three sub-areas of the Adriatic-Ionian domain (ADR1: blue, ADR2: red and IONIAN: green) in the period 1999-2018

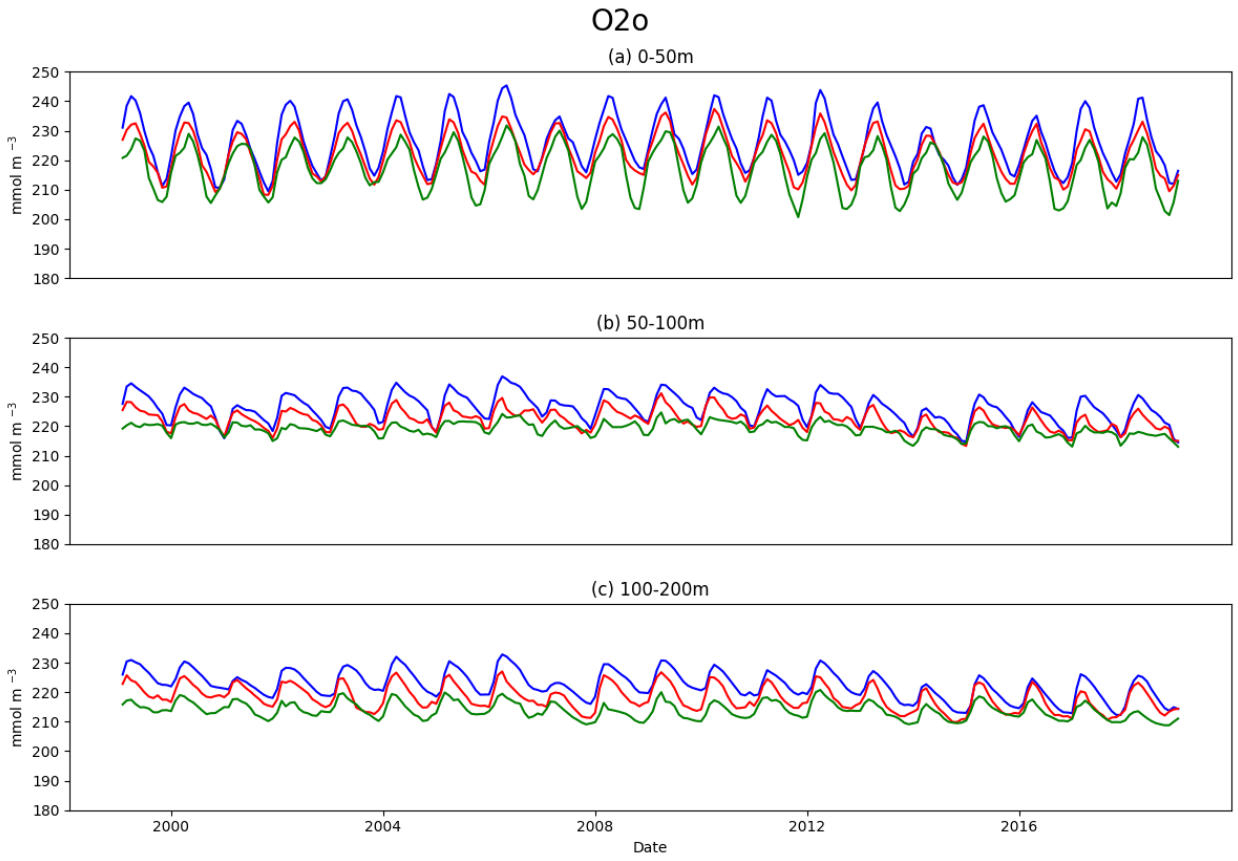

Figure 47 - Monthly timeseries of dissolved oxygen (mmol/m^3) in the inshore zones (depth less than 200 m) of the three sub-areas of the Adriatic-Ionian domain (ADR1: blue, ADR2: red and IONIAN: green) in the period 1999-2018

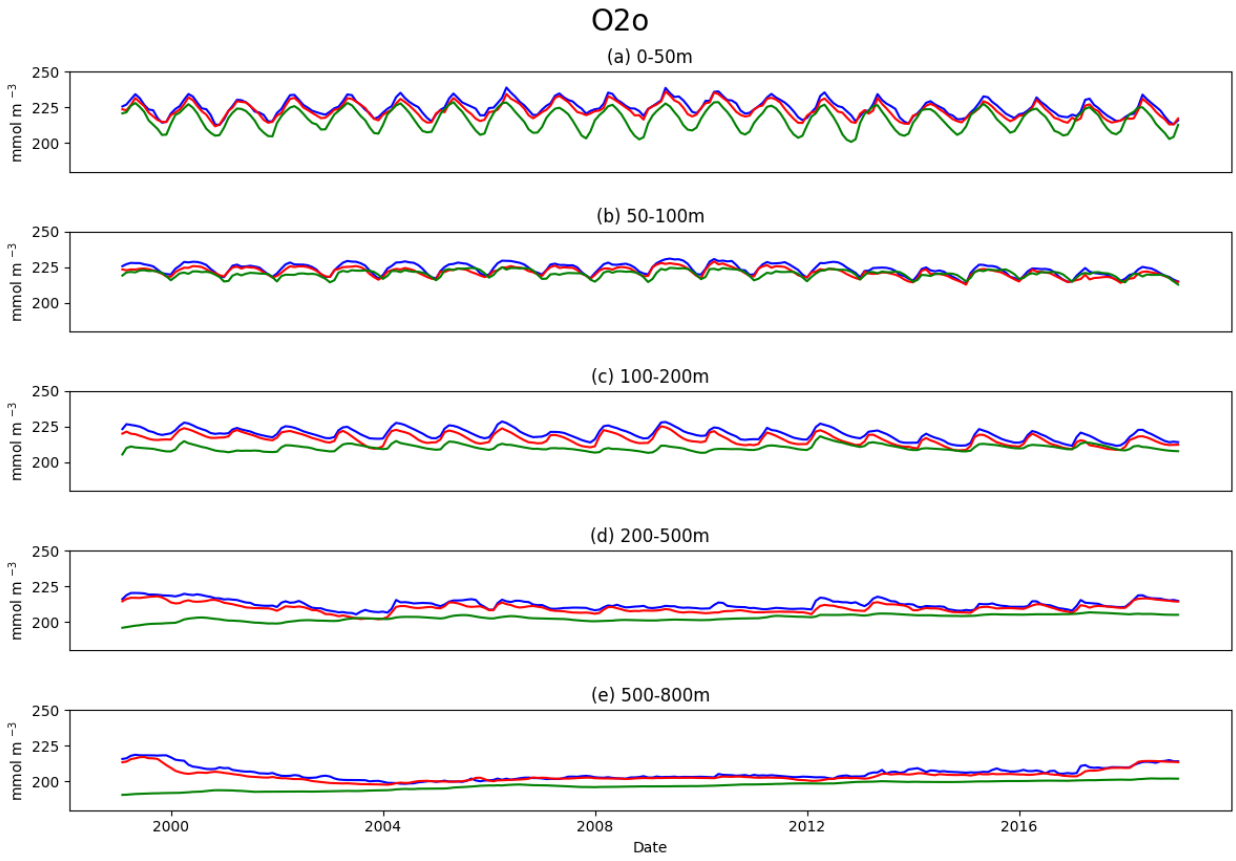

Figure 48 - Monthly timeseries of dissolved oxygen (mmol/m^3) in the offshore zones (deeper than 200 m) of the three sub-areas of the Adriatic-Ionian domain (ADR1: blue, ADR2: red and IONIAN: green) in the period 1999-2018

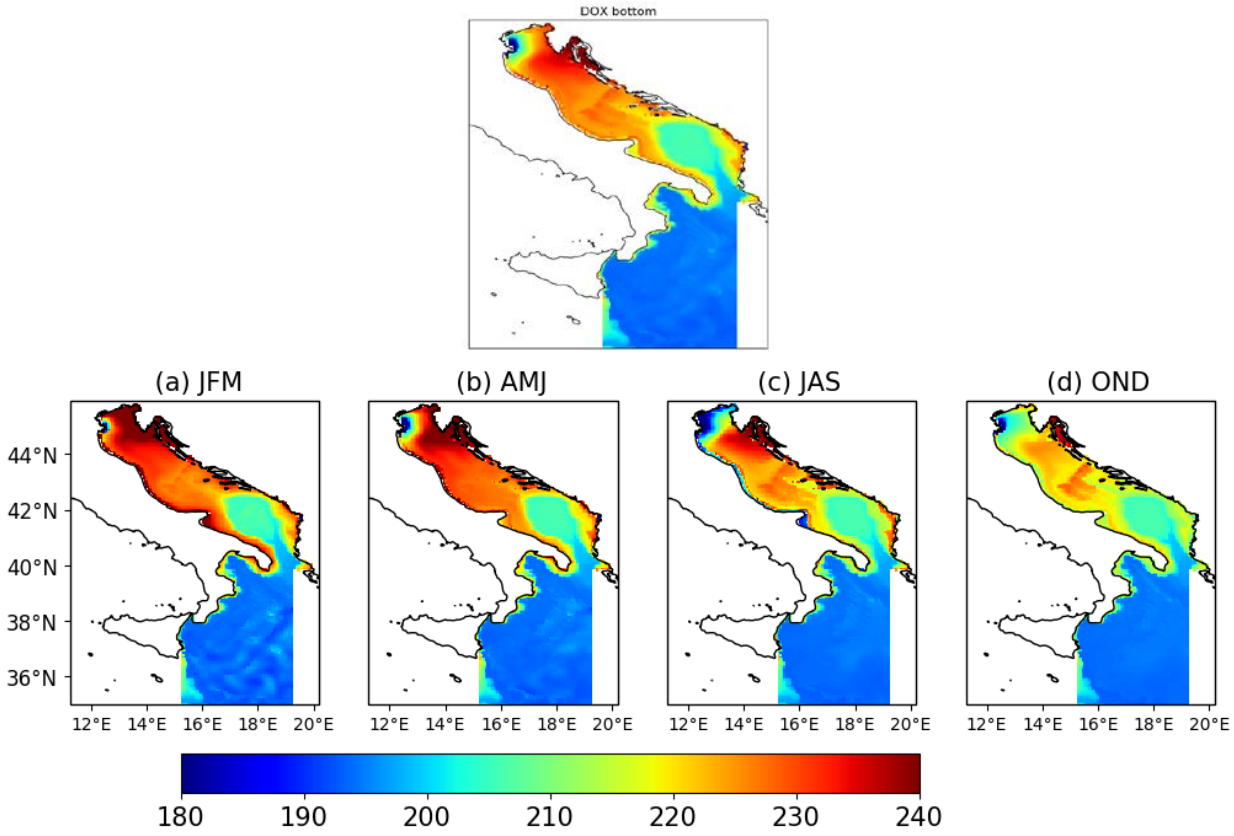

Figure 49 - Mean annual and seasonal concentration (mmol/m^3) of dissolved oxygen at the bottom

Dataset and file format of biogeochemical variables

The original data downloaded from the CMEMS portal have been processed as described in the previous sections. The resulting statistics have been organized in NetCDF files for the specific implementation of the integrated platform of WP4. The chosen standard (NetCDF) allows for a widespread use of the results in all FAIRSEA work packages. In fact, NetCDF (Network Common Data Form) files are self-describing (i.e., they include information about the data they contain), architecture-independent (i.e., they can be accessed by computers with different ways of storing integers, characters, and floating-point numbers), appendable (i.e., data can be easily appended to a NetCDF dataset) and sharable (i.e., multiple users can simultaneously access the same NetCDF file). NetCDF data can be browsed and analyzed through a number of software, like NCO, IDL, MATLAB, PYTHON, cdo, and ncl.

In the dataset some files are named average_X.nc where X can be DIN (dissolved nitrogen), N1p (phosphate), O2o (dissolved oxygen), PH (pH), ppn (net primary production), PC (phytoplankton carbon biomass), P_l (chlorophyll-a), R6c (particulate organic carbon or POC) and ZC (zooplankton carbon biomass). Each file contains the 3D annual (mean) and seasonal (mean_JFM, mean_AMJ, mean_JAS and mean_OND) averages, and the 2D annual and seasonal averages for X between 0-50 m (for example mean_0m_50m), between 50-100 m (for example mean_JFM_50m_100m), between 100-200 m (for example mean_AMJ_100m_200m), between 200-500 m (for example mean_AMJ_200m_500m) and between 500-800 m (for example mean_AMJ_500m_800m). Each file has a dimension of 75 MB. Table 1 shows the dimensions and variables included in the NetCDF files.

Dimensions	VARIABLES		
lon=144	NAME	DIMENSIONS	TYPE
lat=176	Lon	lon	Float32
depth=72	Lat	lat	Float32
	Depth	depth	Float32
	mean	depth,lat,lon	double
	mean_0m_50m	lat,lon	double
	mean_50m_100m	lat,lon	double
	mean_100m_200m	lat,lon	double
	mean_200m_500m	lat,lon	double
	mean_500m_800m	lat,lon	double
	mean_JFM	depth,lat,lon	double
	mean_JFM_0m_50m	lat,lon	double
	mean_JFM_50m_100m	lat,lon	double
	mean_JFM_100m_200m	lat,lon	double
	mean_JFM_200m_500m	lat,lon	double
	mean_JFM_500m_800m	lat,lon	double
	mean_AMJ	depth,lat,lon	double
	mean_AMJ_0m_50m	lat,lon	double
	mean_AMJ_50m_100m	lat,lon	double
	mean_AMJ_100m_200m	lat,lon	double
	mean_AMJ_200m_500m	lat,lon	double
	mean_AMJ_500m_800m	lat,lon	double
	mean_JAS	depth,lat,lon	double
	mean_JAS_0m_50m	lat,lon	double
	mean_JAS_50m_100m	lat,lon	double
	mean_JAS_100m_200m	lat,lon	double
	mean_JAS_200m_500m	lat,lon	double
	mean_JAS_500m_800m	lat,lon	double
	mean_OND	depth,lat,lon	double
	mean_OND_0m_50m	lat,lon	double
	mean_OND_50m_100m	lat,lon	double
	mean_OND_100m_200m	lat,lon	double
	mean_OND_200m_500m	lat,lon	double
	mean_OND_500m_800m	lat,lon	double

Table 1 - Dimensions and variables included in the NetCDF files

In the dataset, some other files are named average_Xbottom.nc where X can be O2o, dissolved oxygen on the bottom. Each file contains the 2D annual and seasonal averages for X on the bottom (for example mean_JAS). Each file has a size of 1 MB. Table 2 shows the dimensions and variables included in these NetCDF files.

Dimensions	**VARIABLES**		
lon=144 lat=176	NAME	DIMENSIONS	TYPE
	Lon	lon	Float32
	Lat	lat	Float32
	mean	lat,lon	double
	mean_JFM	lat,lon	double
	mean_AMJ	lat,lon	double
	mean_JAS	lat,lon	double
	mean_OND	lat,lon	double

Table 2 - Dimensions and variables included in the NetCDF files

References

Dee, D. P., S. M. Uppala, A. J. Simmons, P. Berrisford, P. Poli, S. Kobayashi, U. Andrae et al. "The ERA-Interim reanalysis: Configuration and performance of the data assimilation system." Quarterly Journal of the Royal Meteorological Society 137, no. 656 (2011): 553-597.

Fekete, B.M., C.J. Vorosmarty, and W. Grabs, 1999. Global Composite Runoff Fields on Observed River Discharge and Simulated Water Balances, Tech. Rep. 22, Global Runoff Data Centre, Koblenz, Germany.

Kourafalou, V. H. and Barbopoulos, K.: High resolution simulations on the North Aegean Sea seasonal circulation, Ann. Geophys., 21, 251-265, https://doi.org/10.5194/angeo-21-251-2003, 2003.

Lazzari, P., Solidoro, C., Salon, S., Bolzon, G., 2016. Spatial variability of phosphate and nitrate in the Mediterranean Sea: a modelling approach. Deep Sea Research I, 108, 39-52.

Ludwig W., Dumont E., Meybeck M., Heussner S., 2009. River discharges of water and nutrients to the Mediterranean and Black Sea: Major drivers for ecosystem changes during past and future decades?. Prog. Oceanogr., 80 (3-4): 199-217.

Teruzzi A., Dobricic S., Solidoro C., Cossarini G. 2013. A 3D variational assimilation scheme in coupled transport biogeochemical models: Forecast of Mediterranean biogeochemical properties, Journal of Geophysical Research, doi:10.1002/2013JC009277.

Teruzzi A., Bolzon G.,Salon S.,Lazzari P.,Solidoro C,Cossarini G. 2018 Assimilation of coastal and open sea biogeochemical data to improve phytoplankton simulation in the Mediterranean Sea Ocean Modelling https://doi.org/10.1016/j.ocemod.2018.09.007